REPORT R-1812

NEW FUNDAMENTAL MECHANISM FOR AN ENERGY CONVERSION DEVICE

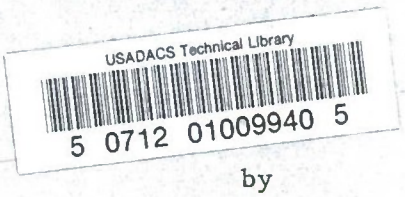

by

FRANK T. PISANO

April 1966

AMCMS Code 5010.11.844

Distribution of this report is unlimited.

UNITED STATES ARMY
FRANKFORD ARSENAL
PHILADELPHIA, PA.

DISPOSITION INSTRUCTIONS

Destroy this report when it is no longer needed. Do not return it to the originator.

The findings in this report are not to be construed as an official Department of the Army position unless so designated by other authorized documents.

REPORT R-1812

NEW FUNDAMENTAL MECHANISM FOR AN ENERGY CONVERSION DEVICE

By

FRANK T. PISANO

AMCMS Code 5010.11.844

Propellant Actuated Devices Division
Components Engineering Directorate
FRANKFORD ARSENAL
Philadelphia, Pa. 19137

April 1966

FOREWORD

The research described in this report was performed by Frankford Arsenal, U.S. Army Munitions Command, Philadelphia, Pa., and was sponsored by the "In-house Laboratory Initiated R&D." The work was accomplished under AMS 5010.11.844, dated 1 July 1962, and was under the supervision of Henry Kahn and, later, George White, of the Pitman-Dunn Research Laboratories.

The program was conducted from 1 July 1962 to 31 July 1965. It was directed by the Propellant Actuated Devices Division of the Components Engineering Directorate, Frankford Arsenal, under the supervision of Frank T. Pisano, Project Engineer and Chief Investigator.

ABSTRACT

This report summarizes the theoretical and experimental studies conducted on a hot gas motor, a fundamentally new mechanism, as an energy conversion device.

In the theoretical study, the relationship of the working components was determined and optimized for maximum conversion of fluid potential and kinetic energy into useful mechanical work. A test model of the hot gas motor was fabricated and a limited series of test runs was conducted, using both cold and hot gas.

This report also presents a design discussion, a vector analysis, and test data of this novel motor.

TABLE OF CONTENTS

List of Illustrations

GLOSSARY

a	Roller piston radius (in.)
$\bar{a}$	Roller vector radius
A	Scalar quantity reaction force between roller and housing
$\bar{A}$	Reaction force vector between roller and housing
b	Rotor radius (in.)
$\bar{b}$	Fixed vector distance between rotor center and the edge of the two ramps
B	Scalar quantity
$\bar{B}$	Reaction force vector between rotor and roller
c	Number of cam surfaces in the housing
$\bar{c}$	Straight line path vector
C	Energy lost due to friction, heat transfer, fluid leakage, etc.
d	Ratio of a/b
$d\bar{r}$	Path differential when position of the roller is given by the radius vector $\bar{r}$
ds	Path differential
F	Fluid pressure force scalar quantity
$\bar{F}$	Force vector due to fluid pressure
G	Torque scalar quantity (in.-lb)
$\bar{G}$	Torque vector
HP	Horsepower scalar quantity
k	Non-negative scalar, called the curvature of the curve at the point
K	Unit vector normal to the plane R and P for a right hand rule
ℓ	Length of the roller (in.)
m	Weight of roller piston (lb)

$\bar{M}$	Inertial force vector of the roller
n	Number of roller pistons
N	Unit vector directed toward the center of curvature
p	Fluid pressure scalar quantity (lb/sq in.)
P	Unit vector normal (perpendicular) to radial vector R and positive in the direction of rotation
Q	Tangential force scalar quantity
$\bar{Q}$	Tangential force vector acting upon the roller
r	Scalar quantity
$\bar{r}$	Radius vector length
$\dot{\bar{r}}$	Velocity vector of radius vector $\bar{r}$
$\ddot{\bar{r}}$	Acceleration vector of the radius vector $\bar{r}$
R	Unit vector in the direction of radial vector $\bar{r}$
RPM	Revolutions per minute
S	Length of arc
s	Unit length of arc
$\dot{s}$	Scalar quantity indicating speed rate of the roller
$\ddot{s}$	Scalar quantity indicating rate of change of speed for the roller
T	Unit vector tangent to the curve
W	Work, energy scalar quantity
α	Angle for optimum torque
β	Angle from top dead center
θ	Rotor angular displacement
$\dot{\theta}$	Angular velocity of rotor
$\ddot{\theta}$	Angular acceleration of rotor
ρ	Radius of the curve at the point

INTRODUCTION

Need for a High-performance Pneumatic (Hot Gas) Motor System

Military and industrial interest and activity in the field of high-performance pneumatically powered actuation and control devices has steadily increased in the past few years with the development of hypersonic aircraft and missiles, and the advent of the oribiting and re-entry space vehicle. The environmental temperature conditions imposed upon power servo-mechanisms which, for example, control the position of aerodynamic control surfaces, have become increasingly severe.

A second major environmental problem contributing to the current interest in pneumatic devices is that of nuclear radiation. The development of airborne reactor-powered engines, however, discourages the use of heavy shielding. Thus, the choice of radiation-insensitive gas as the working fluid for engine controls is necessitated.

The need for gas-powered devices is not limited solely to instances where environmental conditions are severe. In many short duration applications (such as missile and aircraft escape systems), great savings in space and weight result from the use of combustion gases (produced by a solid or liquid propellant gas generator) to operate auxiliary electrical power generating turbines, control surface actuators, and aircraft escape system components.

It is mentioned briefly here that the choice of the means by which pneumatic power is generated varies widely, depending upon the application. Some examples are: solid or liquid monopropellants, liquid bipropellants, compressed air, hot gas or steam from reactor heat exchangers, and the use of stored high pressure gas. Each system has its own relative merits with regard to gas temperature, cleanliness, storability, safety, and mechanical complexity of the associated hardware.

In the work reported in this document, mechanical design was performed under the assumption that the working hot gas would be delivered from one of the family of PAD gas generators used for inflation, i.e., one supplying a relatively cool gas with a slight amount of contamination.

Summary of Accomplishments

The objective of this program was to determine, theoretically and experimentally, the effects of the component relationship in the energy

conversion device and to optimize this relationship for maximum conversion of the fluid potential and kinetic energy into useful rotating work. The first step toward achieving this objective was to analyze the original experimental model of the device (Figures 1 and 2).

A mathematical model of the forces acting within the device was formulated and programmed for the Univac Solid State 90 Computer. The design parameters of the existing model were utilized in the mathematical model. A test fixture was designed and fabricated which consisted of a direct current generator (or dynamometer) connected through a V-belt drive to a pulley on the motor output shaft (Figure 3). Initially, a high pressure compressor and accumulator (serving as the cold gas source) were used to test the motor.

The original experimental model was tested under a no-load condition. For these tests, the motor started only after manual assistance and operated for about a minute before stalling. This original model was modified by introducing thrust bearings between the rotor and the end plate, removing high spots, and inserting a bronze bushing support for the shaft. On subsequent tests, a slight performance improvement was noted.

Based on a vector analysis study (Appendix A), a second experimental model was designed and fabricated. This model was considerably different from the original model, especially in the valving system. The envelope dimensions of the housing (2.6 by 2.6 by 2.5 inches), the roller piston, and the rotor were the same for both units. In addition, this model had generous radii between the ramp and housing cam surface, as illustrated in Figure 4.

When tested, this second experimental model failed to operate; i.e., the rotor locked in place when the motor was subjected to air pressure. The cam surface in the housing of this experimental model was then modified to the asymmetric contour shown in Figure 4, and a thrust ball bearing was placed between the rotor and the exhaust plate. The motor was then subjected to air pressure, and the rotor rotated with considerable speed.

The motor was mounted on the test fixture and connected to the electrical generator (dynamometer) via the V-belt and pulley. Experimental tests continued with a variable torque load applied to the motor shaft by the dynamometer. Different air pressures (cold gas) were applied to the motor. Test data for the cold gas tests are given in Appendix B. The maximum power developed by the motor was 297.5 watts with 1100 psi at the intake port of the motor.

Tests were then performed with hot gas from an XM18 type generator,* a propellant actuated device. (For these tests, the coolant was removed from the XM18 generator.) Two generators were used, one for each

*Developed to inflate a one-man life raft.

Neg: 36.231.S1661/AMC.63

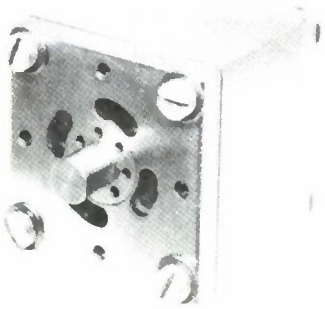

A

Neg: 36.231.S1659/AMC.63

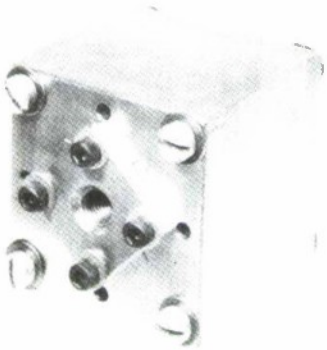

B

Neg: 36.231.S1662/AMC.63

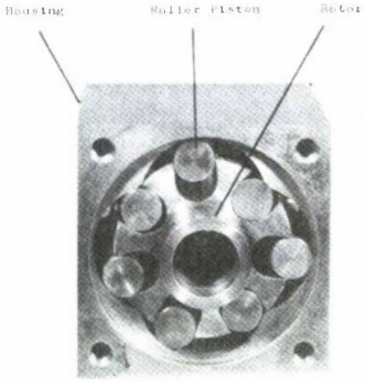

C

Figure 1. A - View of Shaft Output of Mechanism
B - View of Gas Port of Mechanism
C - View of Interior of Mechanism

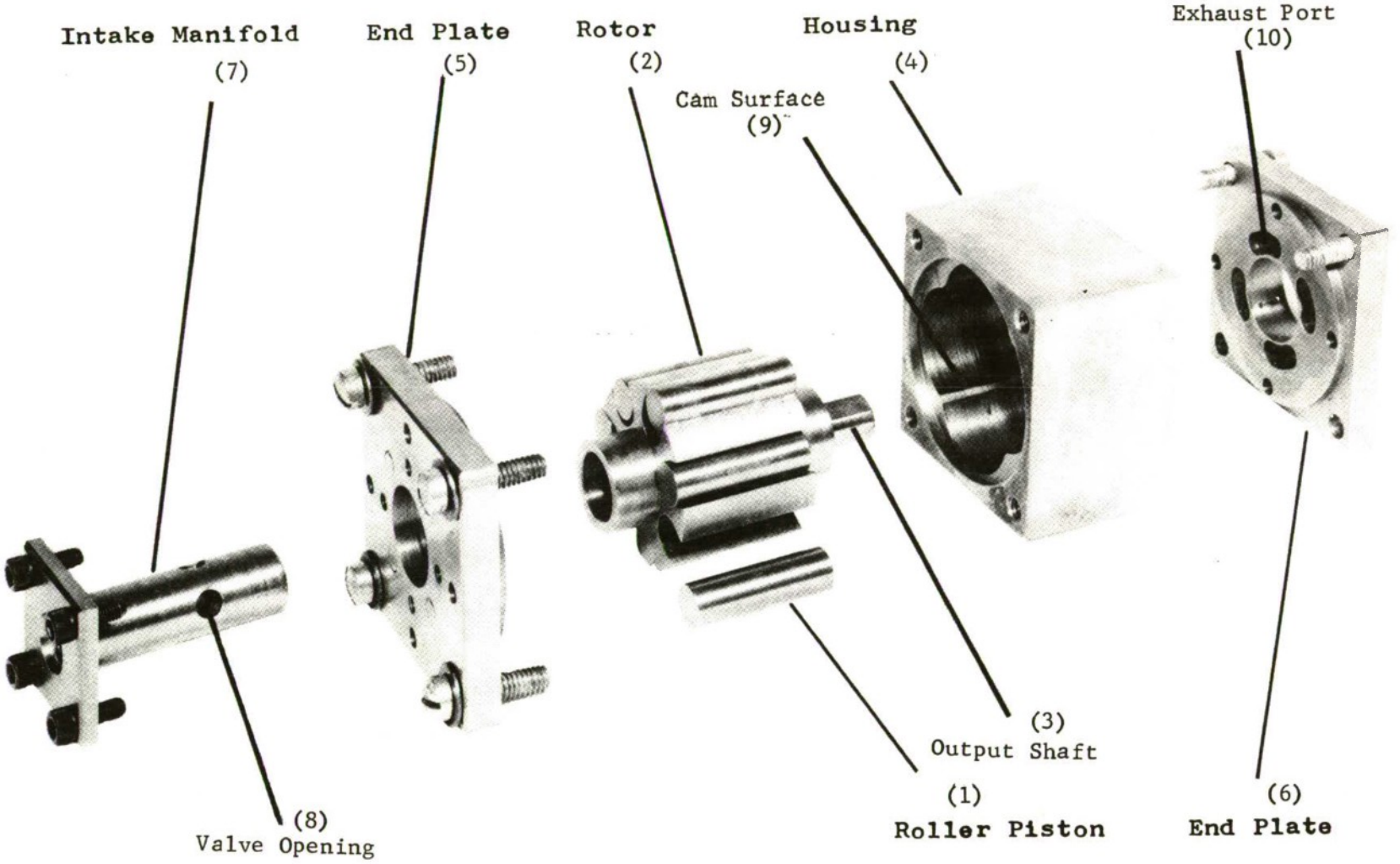

Figure 2. Exploded view of Mechanism

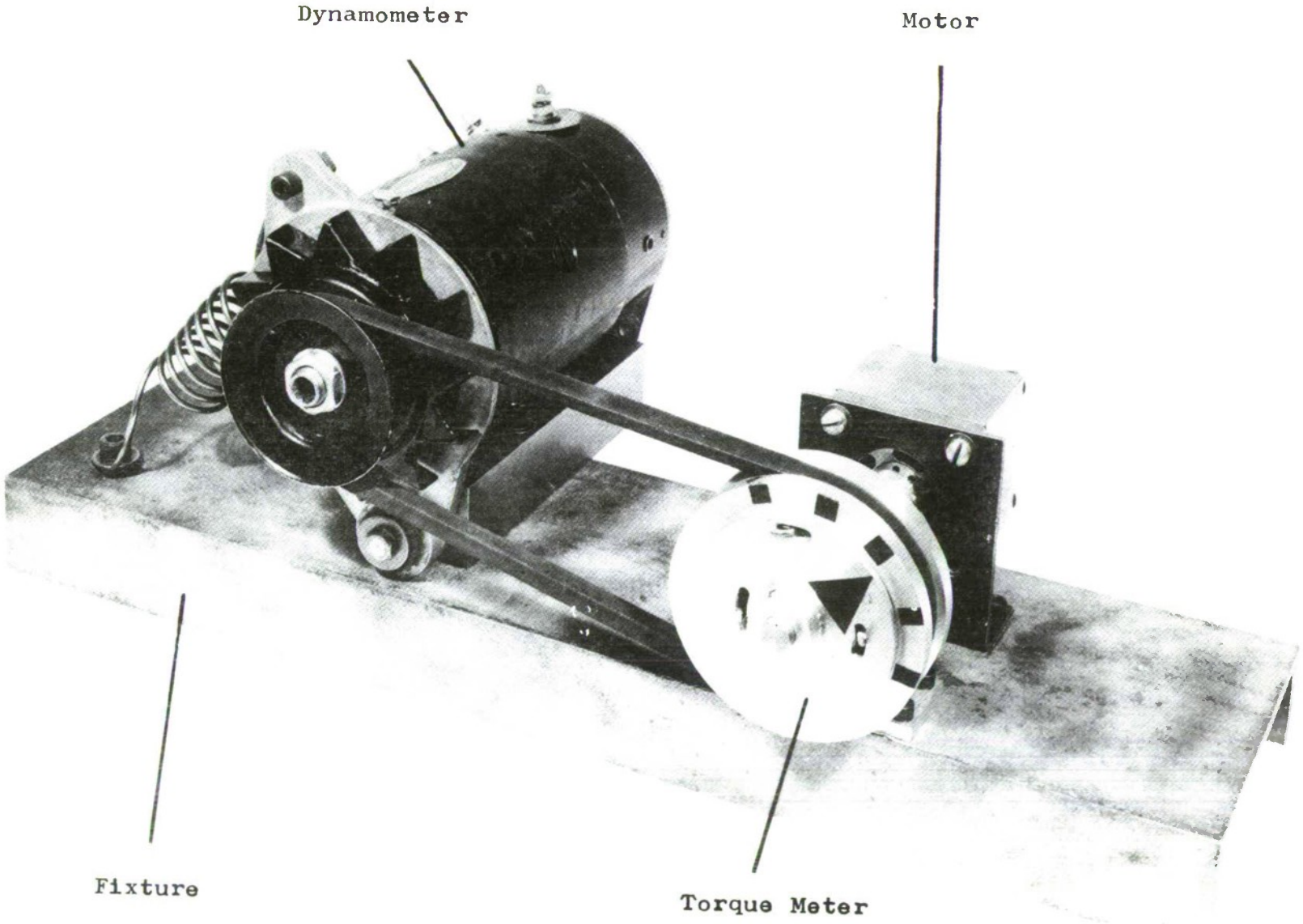

Figure 3. Dynamometer Test Fixture for Mechanism

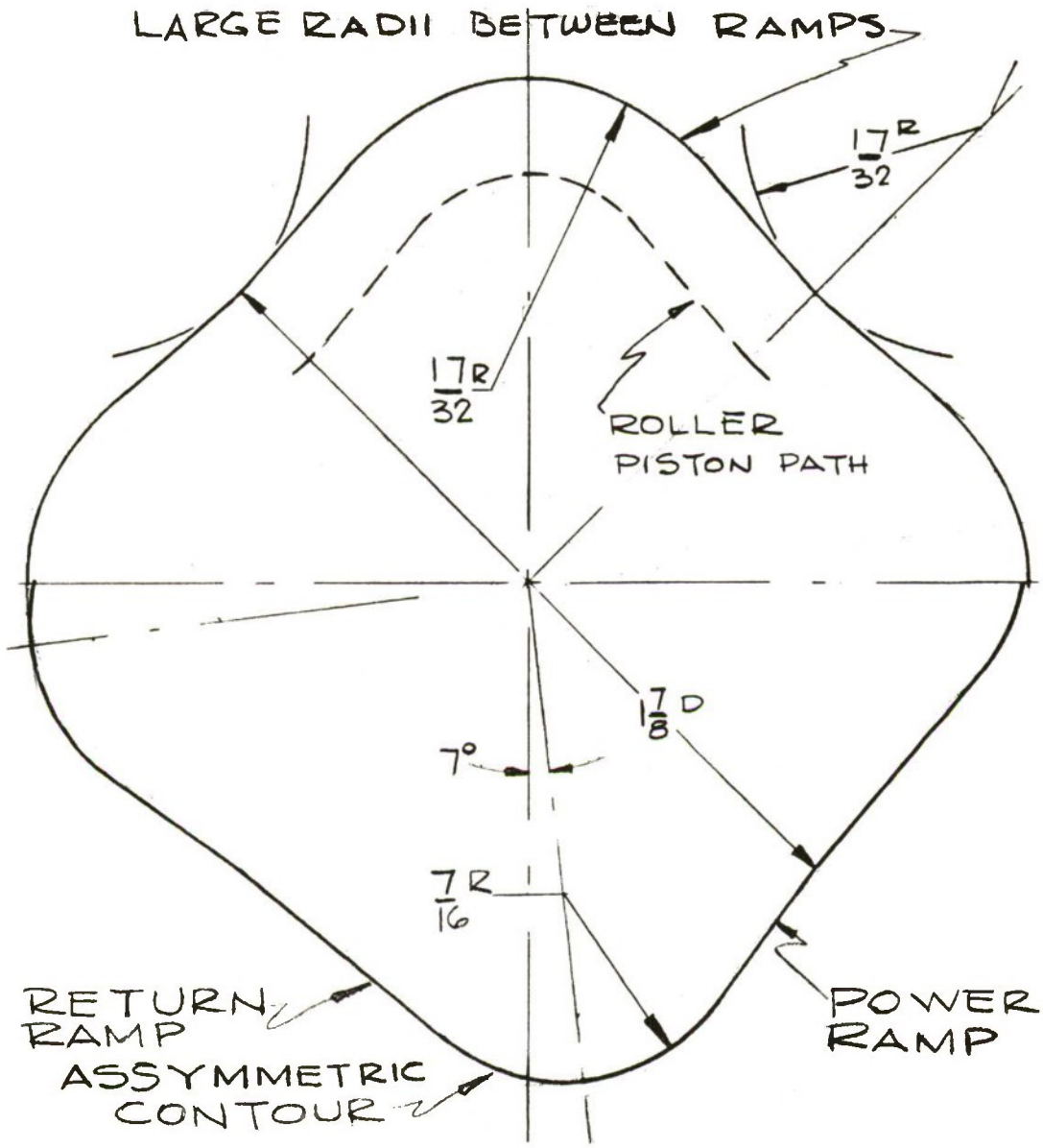

Figure 4. Cam Contours

test run. In each instance, the motor operated for one second (approximately ten revolutions) before stalling. The stalling was apparently due to excessive propellant residue.

It was concluded that the experimental study performed on the modified motor validated the vector analysis.

HISTORICAL BACKGROUND

A feasible hot gas motor (the heart of the system) was required to complete the projected propellant actuated device system for the inertia reel. A search for a motor to meet the desired requirements was unproductive; therefore, a motor which converted fluid energy to a mechanical torque was designed and fabricated.* The experimental model of the motor (shown in Figures 1 and 2) was tested with both compressed and hot gas. As stated, the motor required external cranking to start, and operated for less than a minute.

Theoretically, this fundamental mechanism, which had the potential of operating from a start or stalled condition, was a positive displacement piston engine. Operating on a continuous basis, the mechanism functions like a turbine. When considering the current state-of-the-art, this mechanism had the potential of extremely high output torque for its size ratio.

The total number of working components for the new mechanism was less than that in a positive displacement piston engine, but slightly more than in a turbine. In manufacturing, the new mechanism did not require the exact machining of the turbine blades, and the envelope dimensions, weight, and manufacturing costs were less than for either a turbine or a positive displacement engine.

Very little was known about designing and fabricating this energy-converting device. A theoretical and experimental study was required to obtain design equations for the optimum relationships of the working components for maximum conversion of the fluid potential and kinetic energy into useful mechanical work. Also, some manufacturing knowledge was required as to the fabrication of this device.

*A patent application for this mechanism was submitted, but while the patent search was being conducted, a patent for a very similar motor was awarded to private industry.

THEORY AND OPERATION

Design Discussion

In designing a mechanism, engineering facts and specifications, mathematical equations, and experience are essential. The information supplied in this design discussion satisfies many of these requirements. The conclusions are drawn from the theoretical and experimental studies and fabrication, and the results reflect the most direct solution for establishing design criteria for the objective functional parameters.

Requirements and specifications for an energy conversion device are specified in terms of power and torque output at some designated rotational speed. Usually, these requirements may be calculated from equations utilizing design parameters. The equations presented here (as derived in Appendix A), adhere to the desired procedure and are for ideal conditions, such as a low friction motion and no heat loss.

The following equations cover the dimensions of the working components, based on the given power and torque outputs.

$$HP = \frac{W\ (RPM)}{396{,}000} = \frac{p\ell a^2 nc}{198{,}000}\ (RPM) \qquad (1)$$

(Equation 35, Appendix A)

$$G = \frac{3.69}{RPM}(p_m \ell a)^{3/2} \left(\frac{b}{m}\right)^{1/2} \qquad (2)$$

(Equation 20, Appendix A)

where HP = Horsepower
G = Torque (in.-lb)
p_m = Mean effective pressure (lb/in.^{2})
ℓ = length of the roller piston (in.)
a = Radius of the roller piston (in.)
b = Radius of the rotor (in.)
m = Weight of the roller piston (lb)
RPM = Revolutions per minute
n = Number of roller pistons
c = Number of cam surfaces in the housing.

The design parameters are: (1) the dimensions of the radii of the roller and rotor; (2) the number of rollers in the system; (3) the number of cam surfaces in the housing. In an optimum performance system, these design parameters have an intra-relationship with each other.

The ratio of the radii for the roller to the rotor is expressed by the number of rollers in the system.

$$d = \frac{a}{b} = \frac{\sin\left(\frac{180^\circ}{n}\right)}{1.1 + \sin\left(\frac{180^\circ}{n}\right)} \qquad (3)$$

(Equation 37, Appendix A)

Equation 3 allows for wall thickness in the rotor between the roller slots. In this case, thickness is ten percent of the roller radii. The correlation between the radii of the roller to the rotor can be altered, but this would increase the envelope dimensions of the rotor or decrease the wall thickness between the roller slots.

The equations presented thus far do not satisfy all the parameters. The maximum pressure applied is a function of the yield strength and configuration of the material. As is the practice, it is best to design to a preselected or predesignated pressure to provide a margin of safety. The length of the roller was in the vicinity of four to five times the radius of the roller. The weight of the roller is the product of the density of the material and the volume of the cylinder. Using these figures (which are only guide lines) would facilitate the numerical calculations. However, other factors can be utilized which may prove to be just as suitable.

The number of lobes in the housing is a function of the number of rollers in the system and the angle of inclination, or slopes, of the power ramp. It was determined mathematically that the number of lobes should be one-half the number of rollers. For an odd integer, add one to the number of rollers; for an even integer, add or subtract two. This combination of numbers gives the most satisfactory compromise for design parameters. When both numbers (rollers and lobes) are even, two or more rollers act in unison. If this is the case, the calculated torque should be multiplied by the number of rollers acting in accord. For the calculation of parameters, the torque equation is then divided by this number.

For the optimum torque output, the angle of inclination for the power ramp is derived from

$$\cot(R,T) = \frac{7.8}{RPM}\sqrt{\frac{p\ell a}{m}} \qquad (4)$$

(Equation 19, Appendix A)

This angle should be less than 90°, but greater than the angle whose cosine is $(2 + 3d)/4$.

The slopes of the power and return ramps determine the amount of rotor displacement. A method is presented in Appendix A to design the cam surface (Figure 4) and, also, to determine the rotor power angular

displacement. The rotor angular displacement for the power stroke can be determined from the following equations.

$$\cos\theta = \frac{1}{1 - d}\left\{\cos\beta\,(\cos\beta - 2d) \pm \sqrt{\left[1 - \cos^2\beta\right]\left[1 - \cos^2\beta - 3d^2 - 2d\,(1 - 2\cos\beta)\right]}\right\} \quad (5)$$

(Equation 25, Appendix A)

$$\cos\beta = d\cos^2(R,T) + \sqrt{(1 - d^2) + d^2\left[1 - \cos^2(R,T)\right]^2} \quad (6)$$

(Equation 30, Appendix A)

This displacement angle is limited by the maximum and minimum, as determined by ratio d.

Maximum:
$$\cos\theta = \frac{1 - 2d}{1 - d} \quad (7)$$

(Equation 32, Appendix A)

Minimum:
$$\cos\theta = \frac{(2 + d)(2 - 3d)}{2(1 - d)} - 1 \quad (8)$$

(Equation 31, Appendix A)

The maximum angular displacement of the rotor is attained with the slope of the power ramp at right angle to the radiant. When the roller entrance and arch radii blend, the power ramp is nonexistant and the rotor displacement angle is then at its minimum value.

The return ramp of the cam surface should be tangent to both the arch and rotor (Figure 5). If spacing between lobes is insufficient, the return ramp is shortened and is terminated at the edge of the power ramp of the next lobe. It was found that the slope of the return ramp should be as shallow as possible and the steepness of the slope should never exceed that of the power ramp.

The next design phase to be considered was the fluid flow within the mechanism. In this program, the experimental model was designed to utilize either water, compressed (cold) gas from an accumulator, or hot gas from a PAD gas generator.

In the original experimental model, the intake valve opened as the roller entered the power ramp. In the first modification, the valve opened prior to the roller leaving the return ramp of the preceding lobe. Also, the shape of the valve opening was changed from round to rectangular holes. (The straight edge gave a larger opening quickly.)

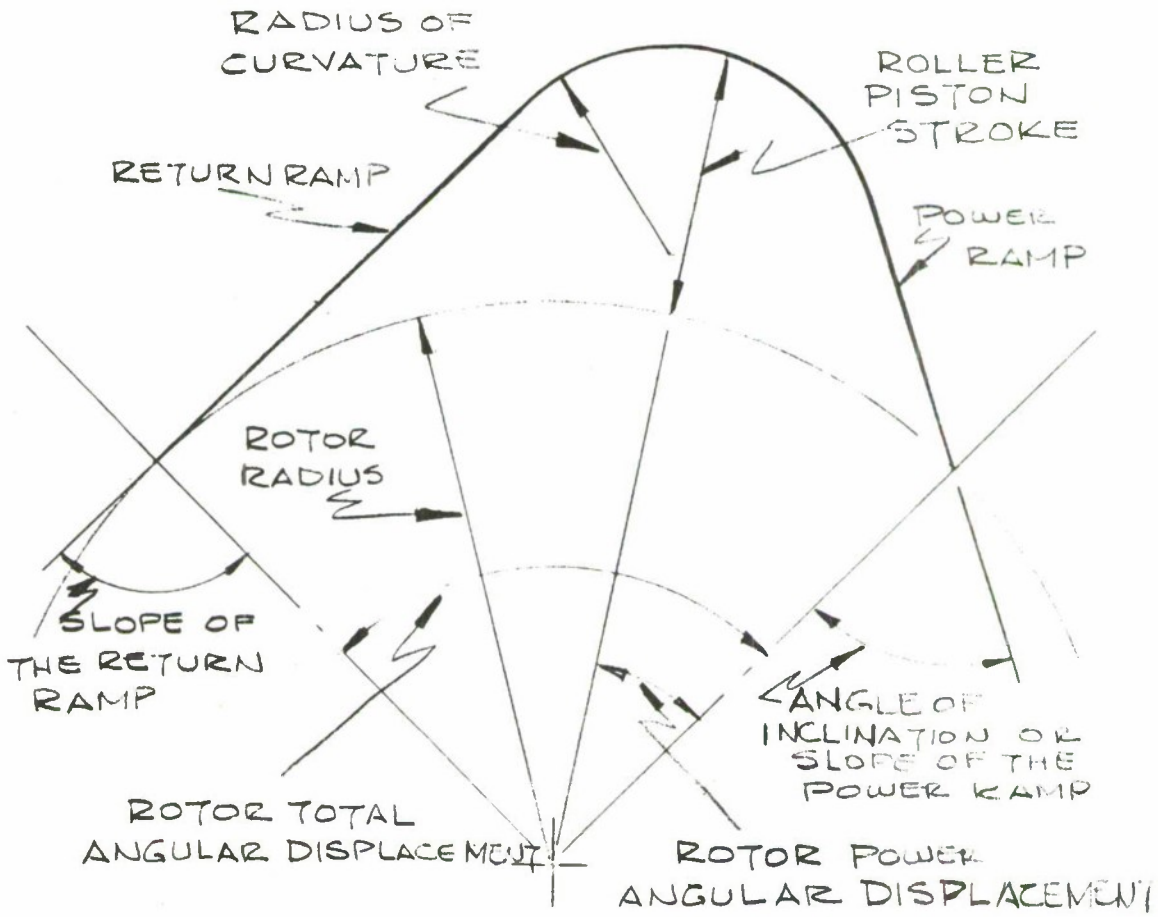

Figure 5. Cam Configuration

The tests showed an improvement in performance. This improvement was due to the higher chamber pressure for the full power stroke and the larger valve opening and connecting passage to the roller chamber. In both models, the intake valve closed near the end of the piston stroke. The energy of the gas expansion was not utilized. To improve the efficiency of converting the gas energy into work energy, the valves should close before the piston stroke is completed.

For both experimental models, the exhaust valve opened after the roller piston had reached its top dead center. The valve had a very large opening. In the second model, the straight edge opening was used, and this was found to be too large. Later, the size of the opening was reduced, resulting in improved performance.

Manufacture of the motor was rather simple, but certain fabrication procedures required specific attention. Close tolerances were held on the following components (see Figures 6 and 7):

1. Roller - diameter, length, and straightness.

2. Rotor - length and width, and straightness of the slot.

3. Shaft - diameter.

4. Bearings - bore diameter.

5. Housing - length, straightness of the cam surface, and parallelism of the plate reference surface.

6. End plates - perpendicularity and eccentricity between bearing bore and reference surface.

The close tolerances on the parts listed above were required to assure the operational performance of the motor. In assembling the mechanism, it was essential that the end plates sit properly. It was found that if one of the plates was slightly cocked, even though not noticeable visually, the mechanism would fail to operate when subjected to air pressure despite the fact that the output shaft appeared to rotate freely. The motor functioned only after the end plates were disassembled and properly reassembled.

For minimum air leakage, the roller and rotor slot must fit closely; also, for good oscillation of the roller within the slot, proper attention during manufacture must be given to the surface straightness, parallelism, and finish of the mating parts.

The shaft and bearing were held to the standard manufacturing tolerances for motors. This also included the alignment of the end bearings and eccentricity of the rotor with respect to the shaft.

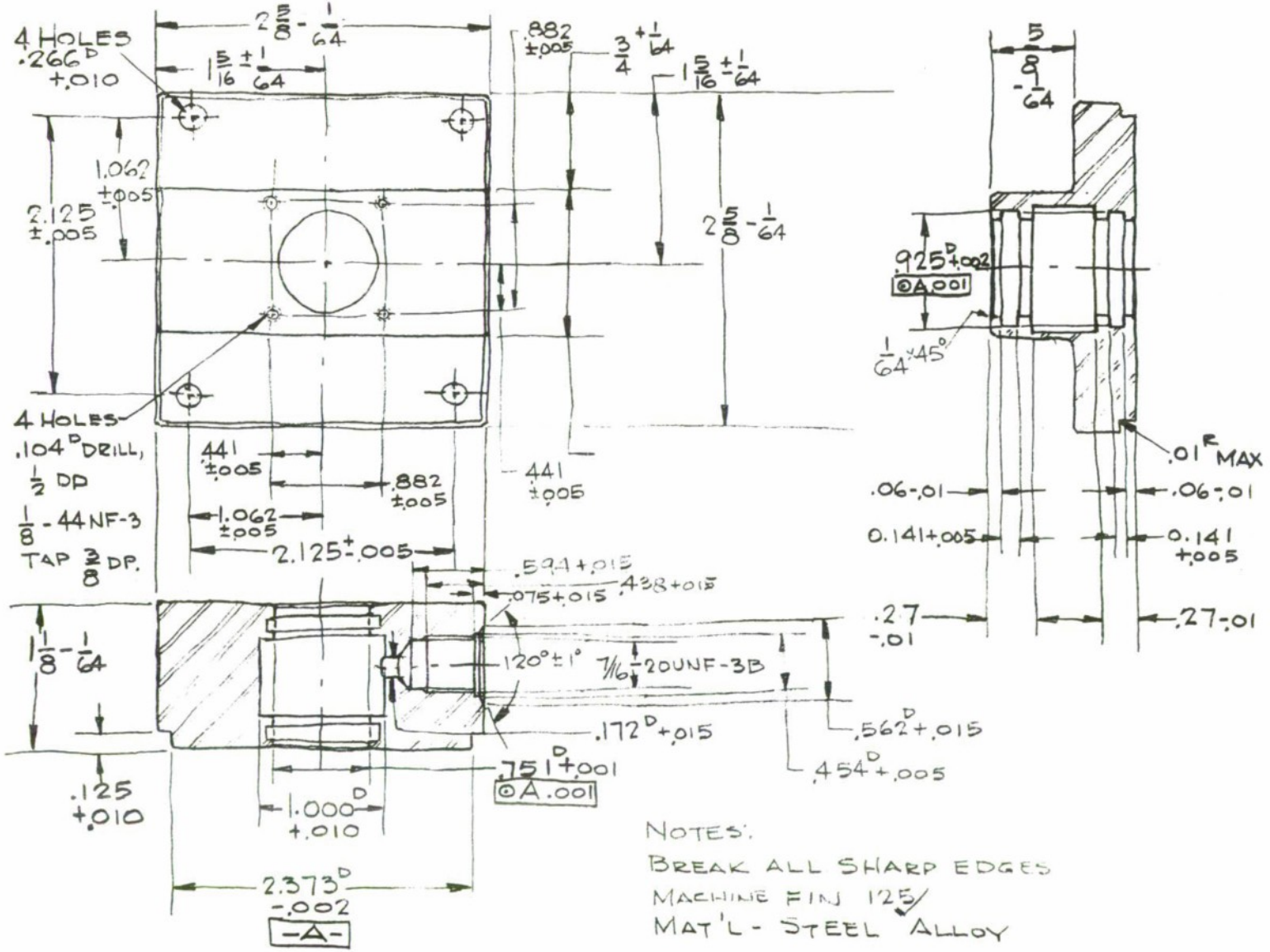

Figure 6. Intake Plate, Energy Conversion Device

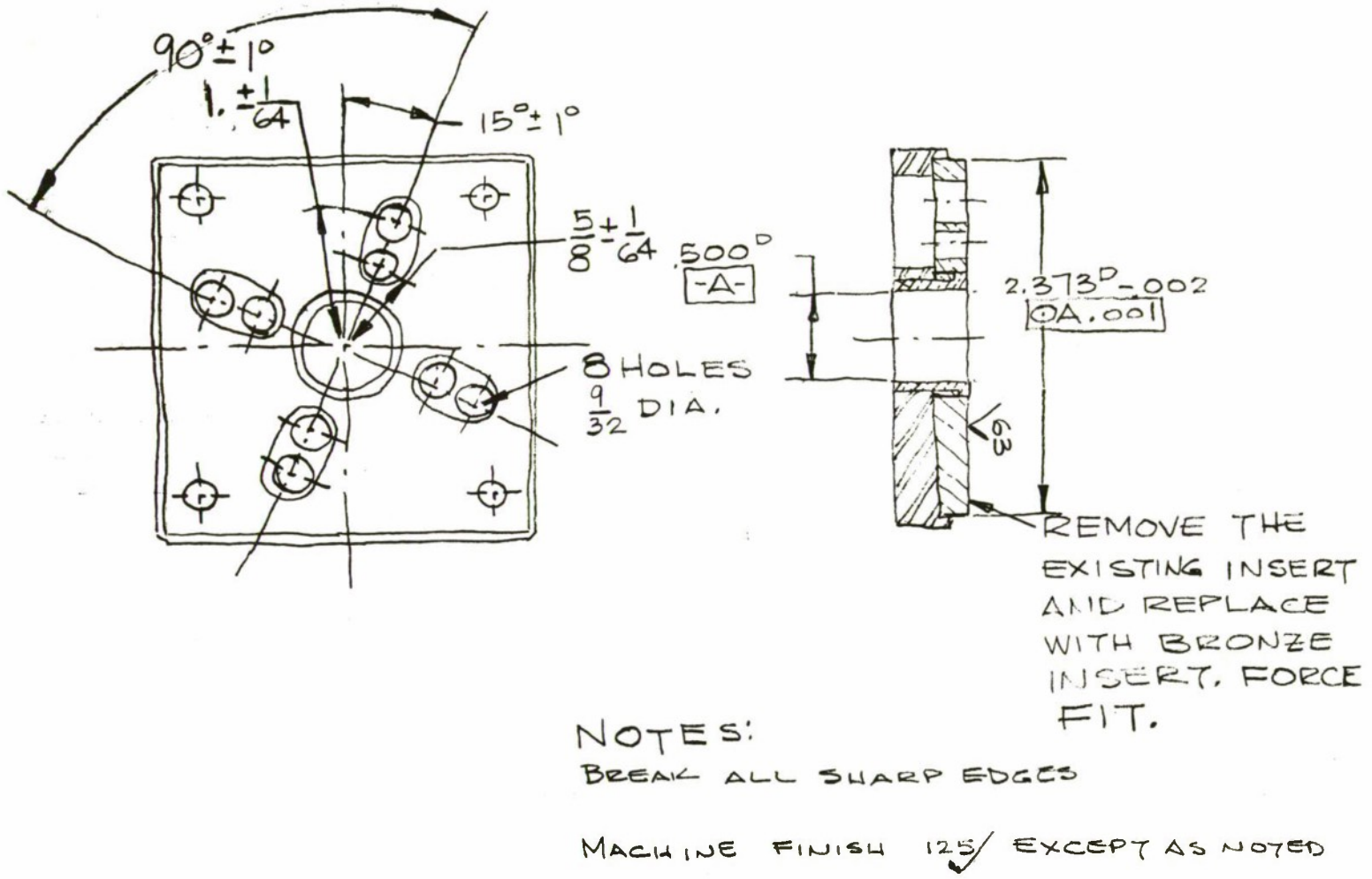

Figure 7. Exhaust Plate, Energy Conversion Device

For extra assurance, the clearance between the housing and rotor included the sum of all the possible tolerances.

Dimension-wise, the cam surface was held within a tolerance of ±0.010 inch. Parallelism and finish were held to standard manufacturing tolerances. The cam surface was inspected after one hour of operation and showed very little wear, which indicated that the roller rotated with little sliding.

Description and Function of the Individual Components

The device was designed to be compact, and improvements were made according to the dictates of the theoretical analysis. The original design (Figure 1, A and B) was fabricated before the analysis was initiated. The components (Figure 2) consisted of an intake manifold, end plates, rotor, roller piston, and housing. In the later experimental model, the intake manifold and asymmetric cam surfaces in the housing were changed (Figures 4 and 8).

The purpose of the intake manifold is to allow the passage of the fluid at the proper time from the source to the internal chamber. The chamber is formed by the rotor, roller piston, and end plates. The intake manifold in the original model (Figure 2) was a cylinder made of steel, with a port in the end plate and four radial valve porting holes. The cylindrical portion fitted into the rotor, which rotated about it. Figure 1B shows the threaded portion for hose connection of the port.

In the second experimental model, the intake manifold was redesigned as shown in Figures 6 and 8. The manifold, which was pivot-supported in the original model, was changed to a shaft bearing in the second model, with subsequent reduction of rubbing surfaces resulting in lower friction. In this redesign, the gas passage was also improved by changing the contour of the valve porting from circular to rectangular, the straight edge of the rectangular shape permitting a quick opening. Also, the opening was positioned to occur sooner by allowing the flow to commence at the end of the return stroke instead of at the beginning of the power stroke.

The steel end plates shown in Figures 1 and 2 support the rotor and seal the ends of the slots in the rotor. The shoulder aligns the end plate with respect to the housing. The eccentricity of the bronze bearing bore is held close for alignment of the shaft and to maintain the rotor clearance with the housing. The intake end plate (Figures 1 and 2) was redesigned to accept the revised intake manifold (Figure 6), while the exhaust plate (Figure 7) was changed to accommodate the change in shaft diameter and smaller exhaust openings.

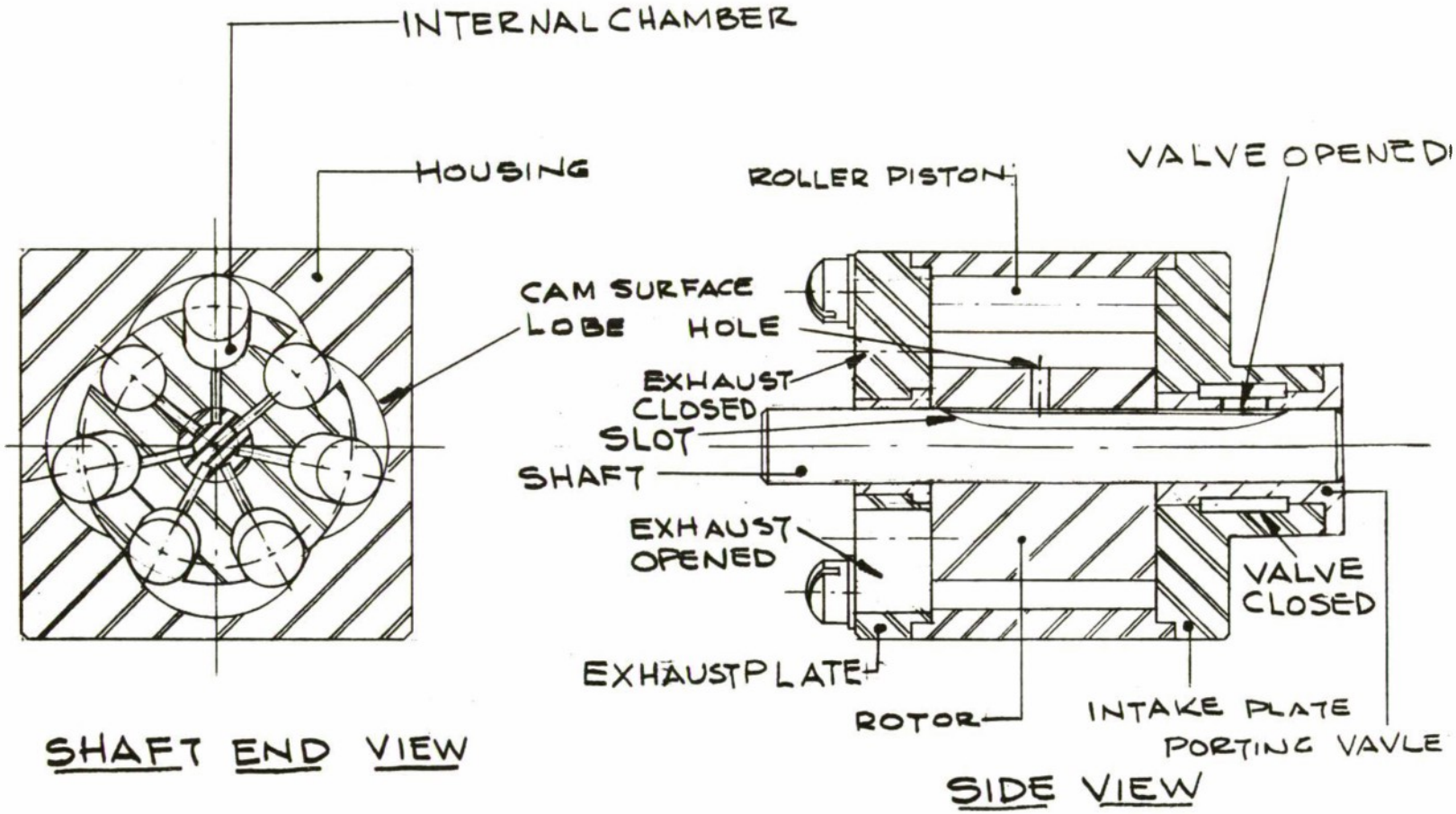

Figure 8. Sectional views, Motor Assembly

The rotor is a cylinder made from steel, with slots cut out for the roller pistons and a shaft (Figures 1C and 2). The slots, end plates, and rollers form a chamber. The seven slots are evenly spaced, and each slot has a clearance with the roller of 0.001 inch minimum and 0.005 inch maximum. A hole at the bottom of the slot, when aligned with the hole in the intake manifold, allows for air passage. The rotor was modified to the new design concept (Figure 9) by reducing rubbing surfaces and friction. The shaft is force-fitted into the rotor, and it has seven elongated slots which, when aligned with the slots in the intake manifold, act as valves for fluid passage.

The roller pistons are solid steel cylinders which act as mechanical barriers to the fluid flow and convert the fluid pressure into a force which is exerted against the cam surfaces of the housing. This force is converted to the power output of the motor. The roller pistons remained the same throughout all modifications.

The housing (Figures 1C and 2) is a block of steel with a cavity, shoulders, cam surfaces, and threaded holes to screw-fasten the end plates. The cam configuration determines the amount and continuity of the torque. The housing underwent two changes of contour in the cam surfaces. The original model was semicircular. The first modification utilized the sinusoidal configuration (Figure 4). The second modification utilized the cam configuration developed in the theoretical analysis. A sketch of the final cam configuration is shown in Figure 5.

The straight line was chosen for the ramp because the roller piston would travel the shortest distance to complete the radial stroke. The straight line portion of the cam surface is comprised of the power and return ramps; the curve portion is the connecting path for the ramps. The slope of the power ramp, upon which the roller strokes outward, converting fluid pressure into torque and power output, is determined by the angle-of-inclination equation. The return ramp is tangent to the arch and to the rotor radius. The arch connects the two ramps for a smooth transition of direction for the roller, and is positioned by the power ramp and maximum height. The maximum height of the curve is the stroking distance of the roller (the radius of the roller) beyond the rotor radius.

Upon completing a cycle (the power and return strokes), the rotor had displaced a fraction of a revolution. This fraction is known as the rotor total angular displacement and is inversely proportional to the number of lobes in the housing. The power angular displacement is determined by the slope of the ramp, which is a function of the number of rollers and lobes.

For the two modifications, the four lobes and stroking height remained the same as in the original model. The final experimental model was designed to the existing parameters of the previous models.

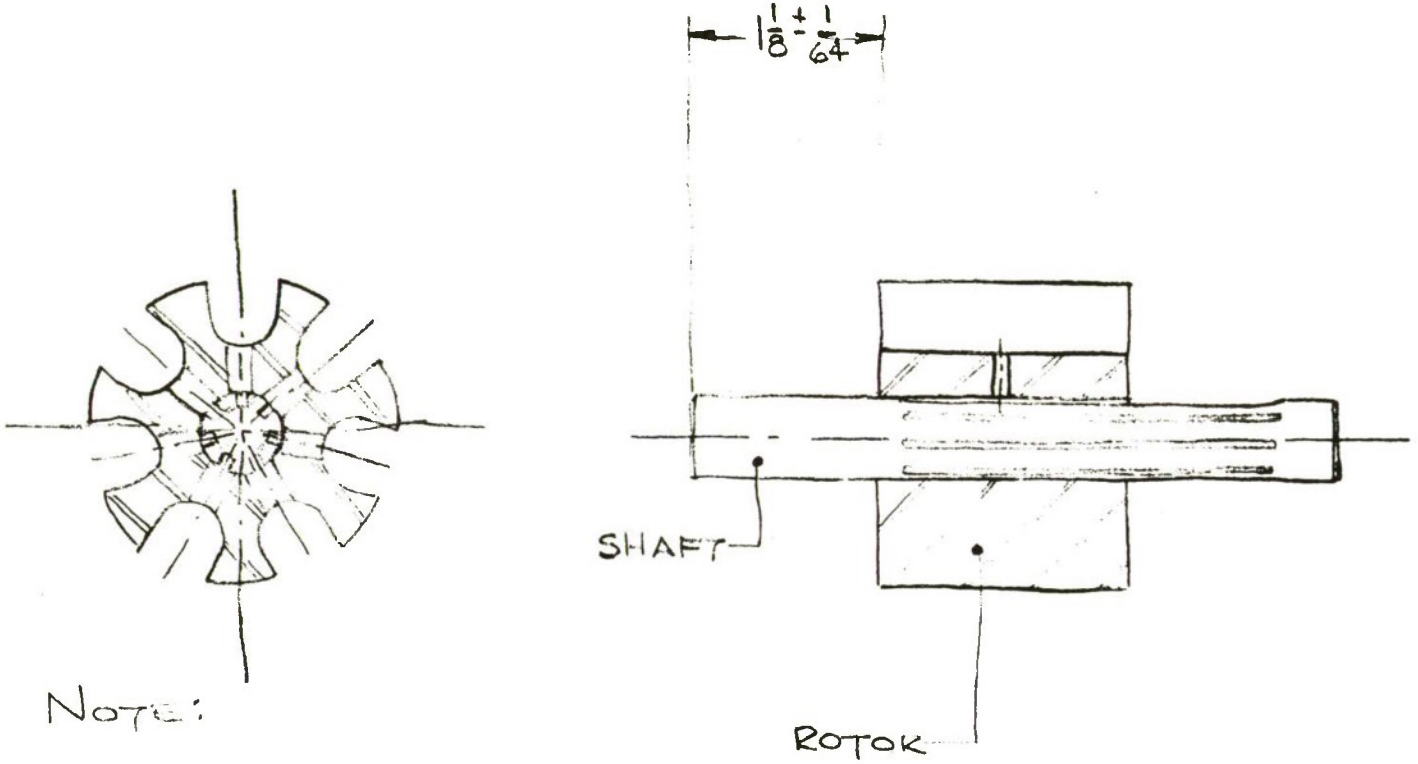

Figure 9. Rotor Assembly, Energy Conversion Device

Operation of Energy Conversion Device

This energy conversion device (Figure 2) is operated by pressurized fluid, which causes the roller pistons (1)* to reciprocate and drive the rotor (2) and output shaft (3). The housing (4), with the two end plates (5,6), contains the working components, and the cam surfaces within the housing determine the travel path of the roller pistons as well as the power and torque output of the motor.

The pressurized fluid (hot or cold gas) enters the intake manifold (7) (see also side view, Figure 8), which has a valve opening (8) to the passage in the rotor, then flows into the chamber formed by the rotor (2), roller (1), and end plates (5,6). When the slot in the shaft (3) aligns with the slot in the valve porting (8), the pressurized fluid flows into the slot of the shaft, then through a hole and slot in the rotor (2). The pressure in the chamber forces the roller piston (1) outward against the power ramp of the cam surface (9). The roller reaction from the power ramp causes the rotor to rotate as long as the roller strokes outward on the power ramp. As the roller (1) approaches the end of the stroke, the intake valve (8) closes, cutting off the supply of fluid. At this point, another roller (1) engages on another power ramp (9) to continue the rotation of the rotor. With the continued motion, the roller piston (1) is carried to the return ramp (9) and exhaust port (10). (Figures 1A and 7 show the exhaust porting.) This port releases the entrapped fluid to the atmosphere. The roller is then returned to the beginning of the stroke and to the power ramp of another cam surface.

The proper placement of the intake and exhaust apertures are essential to the proper operation of the mechanism. To develop maximum torque, full pressure should be applied by opening the valve prior to the power stroke. At some point along the power stroke, the fluid should cease to flow, in order to obtain the most efficient use of the energy from the gas expansion. Of course, if liquid is employed as the pressurized fluid, the flow is continued until the end of the power stroke.

The inclination angle is formed by the ramp and the radius. By reducing the inclination angle, the slope and torque are increased and the angular displacement of the rotor is decreased. The ideal slope would produce the desired torque and maximum angular displacement with the minimum number of roller pistons and lobes.

After the roller completely strokes out, it must return inward to its original position with respect to the rotor. The return ramp is tangent to the rotor, which allows the roller to travel in a straight line without an abrupt change of direction until it enters the power stroke. When the roller leaves the power ramp and enters the return

*Numbers in parentheses refer to Figure 2.

ramp, it goes through a transition path which minimizes the acceleration force of the roller upon the cam surface.

On the return stroke, the fluid trapped within the cavity formed by the rotor, roller piston, and end plates, is evacuated through an outlet opening in the end plate. The position of the outlet is such that the exhaust begins slightly before top dead center of the roller and terminates just prior to the end of the return stroke and intake opening.

The roller has gained kinetic energy at its outermost stroke. This additional kinetic energy is returned to the system as the roller strokes inward. Energy transferred by the pressurized fluid is converted into useful work.

The path which the roller travels is determined by the cam surface (Figure 5). The roller rounds off the sharp corner between return and power ramps, and sharpens the radius of the arch. The shaft end view in Figure 8 shows the roller pistons in various lengths of stroke. The roller pistons reciprocate in the radial direction and function much like a positive displacement engine. As the roller piston and rotor rotate, this gives the flywheel effect of a turbine.

RESULTS AND DISCUSSION

Test Equipment and Instrumentation

The test equipment consisted of rotational and pressure pick-ups. The outputs of these instruments were connected to the electric amplifier and oscillograph.

Experimental Study

The experimental study was conducted to support the results from the vector analysis. The study began with the design and fabrication of the test fixture (Figure 3). An automobile direct-current electrical generator with a 12-volt output was mounted with the gas motor (Figures 1 and 2) on the test fixture. The torque-measuring device with a V-belt connected to the generator was attached to the motor shaft (Figure 3).

Cold Gas (Pressurized Air)

A high-compression air pump and an accumulator with pressure gage, pressure regulator valve, and shut-off globe valve metered the compressed gas to the motor. A hose assembly (AN-4) was connected between the outlet port of the regulator valve and the intake port of the motor. The regulator valve (set at a pressure of 250 psi) was opened, allowing gas to flow to the motor. Under no-load condition (V-belt removed), the shaft revolved only after it was turned manually. The torque developed was insufficient to operate any attachment. In fact, after one minute of operation, the motor stalled.

The next step was to increase the gas pressure to 500 psi and, after a manual start (i.e., hand-cranking), the shaft revolved faster but the torque developed was still insufficient to operate any attachment. The motor was disassembled and inspected for binding. A few high spots were noticed, which indicated signs of wearing between the mating surfaces of the roller and rotor. These high spots were removed by polishing, and a thrust ball bearing was added to the shaft between the rotor and end plate (Figure 2). This modified unit was mounted to the test fixture and retested. The result was a slight improvement in performance, but manual cranking was still required befor the motor operated.

The motor was redesigned, changes being made in: (1) the dimensions and material of the housing; (2) the large radii between the ramps (as shown in Figure 4); and (3) the end plates and rotor assembly (Figures 6, 7, and 9). This unit, the second experimental model (Figure 8), was mounted to the test fixture and the test procedure was repeated, but the motor failed to function. Under air pressure, the shaft locked and could not be turned manually.

The cam surface in the housing of this second model was then modified according to the theoretical analysis shown in Figure 5. This modified second experimental model was then attached to the fixture and subjected to tests. Under various air pressures, the motor performed very satisfactorily. It self-started and operated with high turning speed (2000 rpm) under no-load.

The generator and the torque-measuring device were now attached to the shaft of the motor. Under 500 psi pressure, the motor operated with the attachments. A load of two automobile head lamps was placed in series with the generator armature (or dynamometer). With 750 psi, the gas-driven motor operated the attachments and lighted the lamps. To prevent the bulbs from burning out, the electrical switch was closed for a brief period of time. This final design of the motor was operated several times for durations of five or more minutes with the attachments and lamps.

In comparison, the original model ceased to operate because of rapid wear. The shaft bushing showed the greatest sign of wear. The circular bore hole in the bushing elongated to an almost square shape. The corners of the bore coincided with the corners of the cam surface in the housing. The remaining internal working components showed some signs of wear, but this did not affect the performance.

The final experimental model was subjected to further testing. The air pressure was varied from 300 to 950 psi and the electrical load resistance was varied from 1/2 to 15 ohms. The power output varied from 26 to 298 watts. In this test, an oscillograph was utilized to record the voltage output of the generator, the rotation speed of the motor, and the pressure at the intake port. A resistance type load cell was employed for the pressure pick-up, and a detector light pick-up for the rotation speed. The voltage drop across the resistive load of the generator and the signal voltages of the other two pick-ups were connected to the inputs of an electrical amplifier system. The outputs were connected to the individual recorder of the oscillograph.

Results of this test are also listed in Appendix B.

Hot Gas (XM18 Gas Generator)

For the final test, hot gas from a modified XM18 gas generator was substituted for the compressed air. The XM18 generator was loaded with a charge of approximately 100 grams of RDX propellant. (The chemical coolant normally used for life raft inflation purposes was not used.) A pressure pick-up was attached to the generator to record internal pressure.

In the first ballistic test, the pressures at the generator and intake port were recorded but, due to a malfunction of the instrumentation, rotation of the motor and electrical output of the generator were not recorded. The instruments were adjusted for the second ballistic firing and, prior to the second test, the motor was cleaned of all propellant residue. In the second test, the instrumentation recorded the motor rotation. The gas-driven motor rotated ten complete turns and then stalled. The reason for the stall was excessive accumulation of the propellant gum (or residue of the product of combustion) around the moving parts, causing them to bind to each other. A motion picture camera was used to record both ballistic (hot gas) tests.

CONCLUSIONS

The feasibility of this fundamentally new mechanism for an energy conversion device was demonstrated. Further, the second design model (based on the vector study) proved effective in operating with both cold and hot gas. Thus, the basic concept advanced from the abstract to the feasible.

RECOMMENDATION

It is recommended that studies with this fundamentally new mechanism for an energy conversion device be continued. Particular emphasis should be placed on improving the hot gas performance.

FUTURE WORK

Under the proposed continuation of this project, a range of materials and propellant systems should be selected and evaluated to provide hot gas motor functioning for longer periods of time, i.e., five to ten minutes. It is recognized that the need for such a hot gas energy conversion motor already exists. The basic concept has been demonstrated; design refinement should be completed.

APPENDIX A

VECTOR ANALYSIS OF THE MOTOR

The operational description of the motor has been given in the basic report, but some of it is repeated here to facilitate the vector analysis of the working components in the motor.

Energy is supplied to the motor by a pressurized fluid (liquid, or cold or hot gas). The pressure forces the roller piston through a wedge formed by the housing cam surface and the slot in the rotor, causing the shaft to rotate with a torque. Upon displacing the roller, work is accomplished. The schematic of the working components of the motor and the forces acting upon the roller as a free body are shown in Figure 10.

For this analysis, the equation for work is

$$W_1 = \int_{r_1}^{r_2} \bar{B} \cdot d\bar{r} \tag{1}$$

Here the path differential is called $d\bar{r}$ instead of ds to indicate explicitly that the position of the roller is given by the radius vector $\bar{r}$ with a scalar quantity of the length r.

The sum of the force vectors acting upon the free body is

$$\bar{F} + \bar{B} + \bar{A} + \bar{M} = 0 \tag{2}$$

The fluid pressure force vector $\bar{F}$, due to the construction of the motor, acts in a radial direction. If F is the scalar quantity, the pressure force vector $\bar{F}$ can be identified by FR. R is a unit vector in the direction of the radius vector $\bar{r}$. The rotor reaction force vector $\bar{B}$ acts perpendicularly to the radius vector $\bar{r}$, and the force vector becomes BP. B is the scalar quantity and P is a unit vector perpendicular to the radial vector R and positive in the direction of rotation.

The housing reaction force vector $\bar{A}$ acts normal to the cam surface and through the center of the roller. This force vector is normal to the travel path of the roller. If N is a unit vector directed toward the center of curvature, the vector $\bar{A}$ can be identified by AN where A is the scalar quantity.

The inertial force vector $\bar{M}$ is, by definition, $m\ddot{\bar{r}}$ where m is the mass scalar quantity and $\ddot{\bar{r}}$ is the acceleration force vector of the radius vector $\bar{r}$.

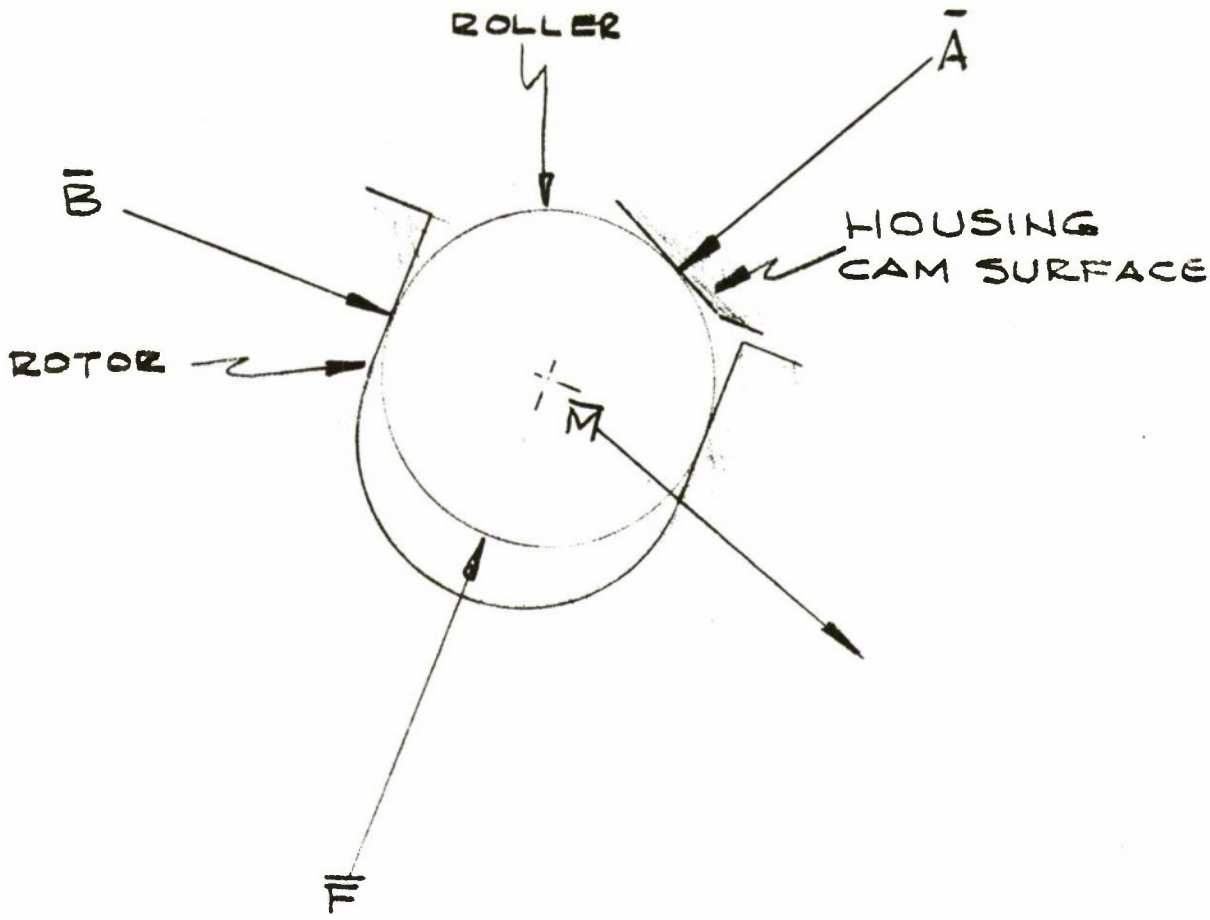

$\bar{A}$ is the reaction force vector between roller and housing.

$\bar{B}$ is the reaction force vector between rotor and roller.

$\bar{F}$ is the force vector due to fluid pressure.

$\bar{M}$ is the inertial force vector of the roller.

Figure 10. Power Stroke Forces acting on the Roller as a Free Body

Substituting the scalar identities into Equation 2,

$$FR + BP + AN - m\ddot{\bar{r}} = 0 \qquad (3)$$

The inertial vector $m\ddot{\bar{r}}$ is opposite to the applied force.

Two of the vectors, N and $\ddot{\bar{r}}$, should be resolved into components with directions to the vectors R and P. The normal of the curve is perpendicular to the tangent of the curve. Before resolving the normal, it is necessary to find the tangent. The tangent to the curve at a point is defined as the limiting position of the secant of the curve between two points as the length of the curve approaches a point or the two points merge. Therefore, $d\bar{r}/ds = T$.

T is a unit vector tangent to the curve. If a unit vector, R, is drawn from the same initial point, O, its end point will describe a circle of unit radius (Figure 11) and the length of arc S is equal to θ. (θ denotes the angle in radians between a fixed line OA and R.) If P is a unit vector perpendicular to R in the direction of increasing angle, it becomes $dR/d\theta = P$.

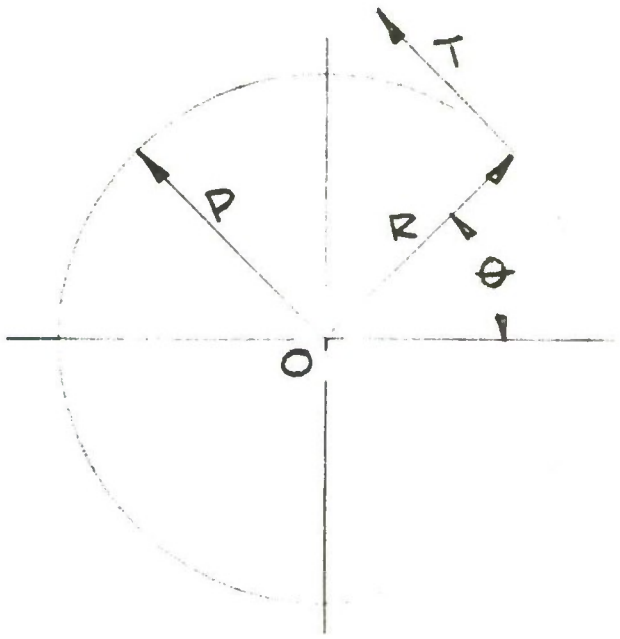

Figure 11. Directions of Unit Vectors

If (r,θ) are the polar coordinates of a point, then the radius vector $\bar{r}$ equals rR where the polar distance r and the unit vector R are functions of θ.

Now,

$$T = \frac{d\bar{r}}{ds} = \frac{dr}{ds} R + r \frac{d\theta}{ds} \frac{dR}{d\theta} = \frac{dr}{ds} R + r \frac{d\theta}{ds} P$$

and

$$R \cdot T = \frac{dr}{ds} ; \qquad P \cdot T = r \frac{d\theta}{ds}.$$

Hence, where ds is a small increment of the path described by the vector $\bar{r}$, $dr/ds = \cos(R,T)$, $r(d\theta/ds) = \sin(R,T)$.

$$T = \cos(R,T)\ R + \sin(R,T)\ P \tag{4}$$

Since T is of constant length, dT/ds, if not zero, must be perpendicular to T.

A directed line through the point of tangency in the direction of dT/ds is called the principal normal of the curve at the point. Let N denote a unit vector in the direction of the principal normal; then, $dT/ds = KN$, where $K(1/\rho)$ is a non-negative scalar called the curvature of the curve at the point. ρ is the radius of the curve at the point.

$$\frac{dT}{ds} = - \sin(R,T)\ R + \cos(R,T) \frac{d\theta}{ds} P + \cos(R,T)\ P + \sin(R,T) \frac{d\theta}{ds} \frac{dP}{d\theta}$$

and

$$\frac{dR}{d\theta} = P = K \times R$$

K is a unit vector normal to the plane R and P for a right hand rule.

$$\frac{dP}{d\theta} = \frac{dK}{d\theta} \times R + K \times \frac{dR}{d\theta}$$

$dK/d\theta$ is opposite in direction to R.

$$\frac{dP}{d\theta} = K \times \frac{dR}{d\theta} = K \times P = -R$$

$$\frac{dT}{ds} = - \sin(R,T)\ R + \cos(R,T) \frac{d\theta}{ds} P + \cos(R,T)\ P - \sin(R,T) \frac{d\theta}{ds} R$$

$$= - \left(1 + \frac{d\theta}{ds}\right) \sin(R,T)\ R + \left(1 + \frac{d\theta}{ds}\right) \cos(R,T)\ P$$

$$= KN$$

if $K = \left(1 + \frac{d\theta}{ds}\right)$.

Then,

$$N = - \sin (R,T)\ R + \cos (R,T)\ P \tag{5}$$

$$\frac{d\ [\cos (R,T)]}{d\ (R,T)} = \cos (R,T + \frac{\pi}{2}) = - \sin (R,T)$$

$$\frac{d\ [\sin (R,T)]}{d\ (R,T)} = \sin (R,T + \frac{\pi}{2}) = \cos (R,T)$$

showing that N is perpendicular to T.

Now, the housing reaction force vector can be written:

$$\bar{A} = AN = A\ [- \sin (R,T)\ R + \cos (R,T)\ P]$$

In the inertial force vector $m\ddot{\bar{r}}$, m is a scalar quantity and the acceleration vector is the second derivative of the radius vector $\bar{r}$ with respect to time.

$$\bar{r} = rR$$

$$\dot{\bar{r}} = \frac{d\bar{r}}{ds}\frac{ds}{dt} = \dot{s}T$$

$\dot{s}$ is a scalar quantity which is the speed rate of the roller on the curve.

$$\ddot{\bar{r}} = \ddot{s}T + \frac{\dot{s}^2}{\rho} N$$

The scalar quantity $\ddot{s}$ indicates the rate of change of speed for the roller traveling on its path.

Substituting in Equations 4 and 5,

$$\ddot{\bar{r}} = \ddot{s}\ [\cos (R,T)\ R + \sin (R,T)\ P] + \frac{\dot{s}^2}{\rho}\ [- \sin (R,T)\ R + \cos (R,T)\ P]$$

Replacing the terms in Equation 3,

$$FR + BP + A\ \{-\sin (R,T)\ R + \cos (R,T)\ P\} - m\{\ddot{s}\ [\cos (R,T)\ R + \sin (R,T)\ P]$$

$$+ \frac{\dot{s}^2}{\rho}\ [-\sin (R,T)\ R + \cos (R,T)\ P]\} \tag{6}$$

Multiplying Equation 6 by $\cdot P$, the rotor reaction scalar quantity is

$$B = -A \cos (R,T) + m[\ddot{s} \sin (R,T) + \frac{\dot{s}^2}{\rho} \cos (R,T)] \tag{7}$$

Multiplying Equation 6 by $\cdot R$,

$$A = \frac{1}{\sin (R,T)} \left\{-m \left[\ddot{s} \cos (R,T) - \frac{\dot{s}^2}{\rho} \sin (R,T)\right] + F\right\}$$

Introducing this equation into Equation 7,

$$B = F \cot (R,T) - \frac{m\ddot{s}}{\sin (R,T)} \tag{8}$$

Substituting Equation 8 into Equation 1,

$$W_1 = \int_{r_1}^{r_2} F\dot{s} \cos (R,T) - m\ddot{s}\dot{s}.$$

The scalar quantity $\dot{s}$ is a function of $\sqrt{\dot{\bar{r}} \cdot \dot{\bar{r}}}$, or $|\dot{\bar{r}}|$, or it is a function of the radius scalar quantity r.

$$W_1 = \int_{r_1}^{r_2} F\dot{s} \cos (R,T) - \int_{\dot{s}_1}^{\dot{s}_2} m\ddot{s}\dot{s}$$

$$W_1 = F (r_2 - r_1) - \frac{m}{2} (\dot{s}_2^2 - \dot{s}_1^2) - C_1 \tag{9}$$

$(r_2 - r_1)$ is the roller radial displacement (or stroke) and $m\dot{s}^2/2$ is the kinetic energy of the roller. C_1 is the energy lost due to friction, heat transfer, fluid leakage, etc.

When the roller piston is at the end of the stroke, or furthest away from the rotor center of rotation, the roller possesses additional kinetic energy above that at the beginning of the stroke. To return this roller to the initial radial position may require additional energy (which can be taken from the system) or it may return some of its kinetic energy to the system. On the return stroke, the fluid pressure force, $\bar{F}$, is omitted and the remaining force vectors are positioned as shown in Figure 12.

Now, $\bar{B} + \bar{M} + \bar{A} = 0$. Substituting the scalar quantity and unit vector, $BP + m\ddot{r} + AN = 0$,

$$BP + m (\ddot{s}T + \frac{\dot{s}^2}{\rho}N) + AN = 0.$$

Multiplying by $\cdot T$,

$$BP \cdot T = -m\ddot{s}$$

$$B \sin (R,T) = - m\ddot{s}$$

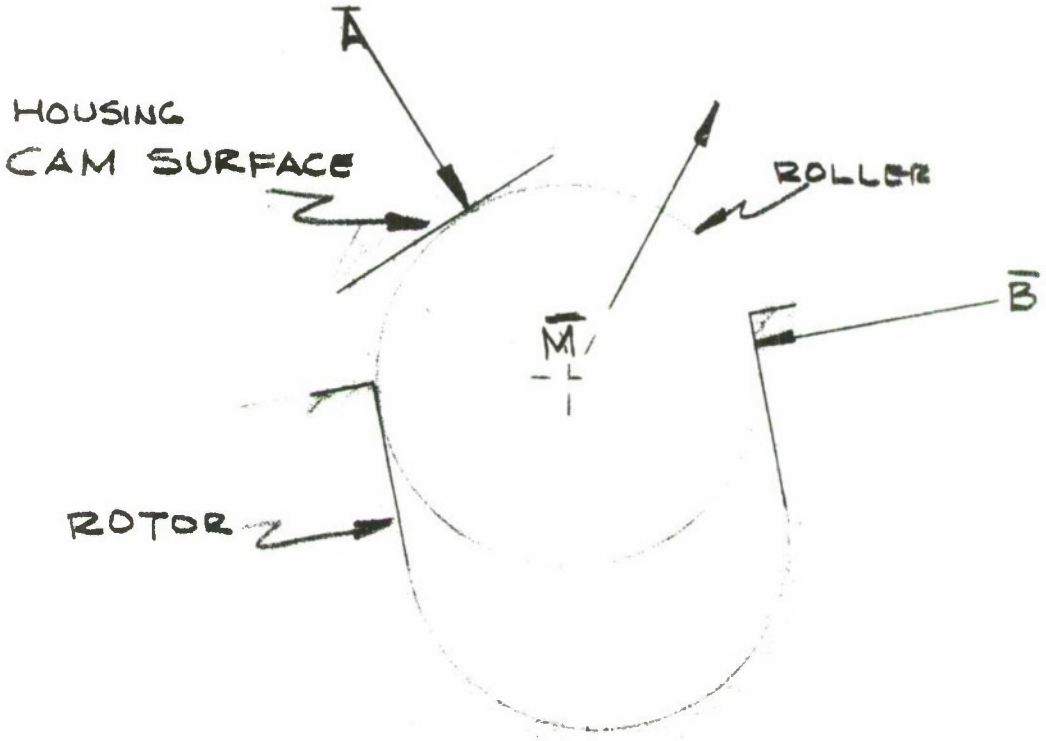

Figure 12. Return Stroke Forces Acting on Roller as a Free Body

$$B = - \frac{m\ddot{s}}{\sin (R,T)} \tag{12}$$

Substituting B (Equation 12) into the work equation,

$$W_2 = \int_{r_2}^{r_1} - \frac{m\ddot{s}}{\sin (R,T)} P \cdot d\bar{r}$$

$$= - \int_{r_2}^{r_1} \frac{m\ddot{s}}{\sin (R,T)} P \cdot \dot{s} \left[\cos (R,T)\ R + \sin (R,T)\ \dot{P}\right]$$

$$= - \int_{r_2}^{r_1} m\ddot{s}\dot{s} = - \int_{s_2}^{s_1} m\ddot{s}\dot{s} = - \frac{m}{2} (\dot{s}_1^2 - \dot{s}_2^2) - C_2$$

$$W_2 = \frac{m}{2} (\dot{s}_2^2 - \dot{s}_1^2) - C_2 \tag{13}$$

As the speed of the roller is greater at the beginning of the return stroke, some of the kinetic energy is converted to work. Therefore, the total shaft output for a cycle is the sum of the work accomplished by the roller in the power and return strokes.

$$W_T = W_1 + W_2$$

$$= F(r_2 - r_1) - \frac{m}{2}(\dot{s}_2^2 - \dot{s}_1^2) + \frac{m}{2}(\dot{s}_2^2 - \dot{s}_1^2) - C_1 - C_2$$

$$W = F(r_2 - r_1) - C \tag{14}$$

The work output of the shaft is the product of the force acting on the roller and its displacement minus the energy loss. The work equation can be derived by utilizing the forces acting tangentially to the path and displacement of the roller. By definition, work done by the roller is

$$W = \int_{r_1}^{r_2} \bar{Q} d\bar{r}$$

$\bar{Q}$ is the tangential force acting upon the roller.

Referring to Figure 11,

$$\bar{M} + \bar{A} + \bar{F} + \bar{Q} = 0$$

$$-m\ddot{\bar{r}} + AN + FR + QT = 0.$$

Multiplying by $\cdot T$,

$$-m\ddot{\bar{r}} + FR \cdot T + Q = 0$$

$$Q = -F \cos(R,T) + m\ddot{s}$$

and

$$d\bar{r} = \dot{s}\frac{\dot{\bar{r}}}{\dot{s}} = \dot{s}T$$

Substituting into the work equation,

$$W = \int_{r_1}^{r_2} F \frac{dr}{ds} T \cdot \dot{s}T - \int_{s_1}^{s_2} m\ddot{s}T \cdot \dot{s}T = \int_{r_1}^{r_2} F\dot{r} - \int_{s_1}^{s_2} m\ddot{s}\dot{s}$$

$$W = F(r_2 - r_1) - \frac{m}{2}(s_2 - s_1) - C_1 \tag{15}$$

The conclusion is that the work done by the roller is transmitted directly to the rotor. The work equation shows that the radial displacement of the roller does the work, and, as far as work is concerned, displacement in any other direction has no significance.

In deriving the work equation, it was found that the force acting on the housing surface is

$$A = \frac{1}{\sin (R,T)} \left\{ F - m \left[\ddot{s} \cos (R,T) - \frac{\dot{s}^2}{\rho} \sin (R,T) \right] \right\}$$

If the rotor is stalled, the maximum force exerted on the housing cam surface by the roller is

$$A = \frac{F}{\sin (R,T)} \tag{16}$$

where F is the pressure force upon the roller, and the angle (R,T) is the angle formed by the radial line and line tangent to the roller path. The force acting upon the surface of the slot in the motor is

$$B = \left[F \cot (R,T) - m\ddot{s} \csc (R,T) \right]$$

When the rotor is stalled, the maximum force exerted is:

$$B = F \cot (R,T). \tag{17}$$

This motor develops torque in performing work. By definition, torque for a single roller piston is

$$\bar{G}_1 = \bar{r}_1 \times \bar{B}_1$$

and, for several roller pistons, it is

$$\bar{G} = \bar{r}_1 \times \bar{B}_1 + \bar{r}_2 \times \bar{B}_2 + \bar{r}_3 \times \bar{B}_3 \ldots\ldots \text{ etc.}$$

Substituting,

$$\bar{G} = r_1 R_1 \times \left[F \cot (R,T) - m\ddot{s} \csc (R,T) \right]_1 P_1 + r_2 R_2 \times \left[m\ddot{s} \csc (R,T) \right]_2 P_2 + \ldots\ldots \text{ etc.}$$

$$\bar{G} = \left[F \cot (R,T) - m\ddot{s} \csc (R,T) \right]_1 r_1 K + \left[m\ddot{s} \csc (R,T) \right]_2 r_2 K + \ldots\ldots \text{ etc.}$$

K is a unit vector perpendicular to R and P plane. In this case, the R and P remain in a single plane, and rotation is about a single line perpendicular to this plane. All the torque vectors are colinear. Therefore, the torque scalar quantity can be added algebraically.

$$\bar{G} = \left\{\left[F \cot (R,T) - m\ddot{s} \csc (R,T)\right]_1 r_1 + \left[m\ddot{s} \csc (R,T)\right]_2 r_2 + \ldots\ldots \text{etc}\right\} K$$

$$\bar{G} = \left\{\csc (R,T)_1 \left[F \cos (R,T) - m\ddot{s}\right]_1 r_1 + \left[m\ddot{s} \csc (R,T)\right]_2 r_2 + \ldots\ldots \text{etc}\right\} K \tag{18}$$

The torque is directly proportional to the cosecant of the angle formed by the radial line and the tangential line. If this angle is held constant,

$$\cot (R,T) = \frac{\dot{r}}{r\dot{\theta}}$$

$$\dot{\theta} \cot (R,T) = \frac{\dot{r}}{r}$$

$$\theta \cot (R,T) = \log r - \log c$$

$$r = ce^{\theta \cot (R,T)}$$

$$\dot{s} = \sqrt{\dot{r}^2 + (r\dot{\theta})^2}$$

$$\dot{s} = r\dot{\theta} \csc (R,T)$$

$$\ddot{s} = r \csc (R,T) \left[\dot{\theta} \cos^2 (R,T) \cot (R,T) + \ddot{\theta}\right]$$

For constant $\dot{\theta}$, $\ddot{\theta}$ is zero, and for $\ddot{s}$ to equal zero, the angle (R,T) is π/a, or 90°. For this angle, the curve is a circle and no torque develops. For the angle (R,T) is zero radian, $\ddot{s}$ is infinitely large and the rotor remains in position. Somewhere between the two extreme angles, the ideal condition exists.

Utilizing the T,N system, the scalar quantity of the torque vector is

$$G = \left[F \cot (R,T) - m\ddot{s} \csc (R,T)\right] r.$$

Utilizing the R,P system,

$$G = \left\{F \cot (R,T) - m\left[\ddot{r} \cot (R,T) + r\ddot{\theta}\right]\right\} r.$$

For a family of curves with constant tangent angle,

$$\tan (R,T) = \frac{r\dot{\theta}}{\dot{r}}$$

$$\dot{r} = r\dot{\theta} \cot (R,T).$$

Differentiating,

$$\ddot{r} = (\dot{r}\dot{\theta} + r\ddot{\theta}) \cot (R,T)$$

$$= \left[r\dot{\theta}^2 \cot (R,T) + r\ddot{\theta}\right] \cot (R,T)$$

Substituting,

$$G = \left\{F \cot (R,T) - m \left[r\dot{\theta}^2 \cot^3 (R,T) + r\ddot{\theta} \csc^2 (R,T)\right]\right\} r.$$

Differentiating this equation with respect to the tangent angle, and holding the other variable constant,

$$\frac{dG}{d(R,T)} = \left[- F + 3mr\dot{\theta}^2 \cot^2 (R,T)\right] r \csc^2 (R,T)$$

For maximum torque, $\frac{dG}{d(R,T)} = 0$, therefore

$$\cot (R,T) = \sqrt{\frac{F}{3mr\dot{\theta}^2}}$$

$$F = 2p\ell a$$

where p = the fluid pressure (lb/sq in.)

ℓ = the length of the roller (in.)

a = the radius of the roller (in.) and $d = a/b$

$2\ell a$ = the piston area of the roller (sq in.)

$\dot{\theta} = \pi/30$ RPM and $r = b$.

$$\cot (R,T) = \sqrt{\frac{600\ p\ell a}{\pi^2 m\ (RPM)^2}} = \frac{7.8}{RPM} \sqrt{\frac{p\ell a}{m}} \qquad (19)$$

As the pressurized fluid, roller diameter, length and weight, and rotational speed are design parameters, the optimized torque can be expressed as

$$G = \frac{3.69}{RPM} (p\ell a)^{3/2} \left(\frac{b}{m}\right)^{1/2} \qquad (20)$$

The work and optimized torque equations illustrate the fact that a radial movement of the roller provides the work energy, and optimum torque is provided at a definite tangent angle. The shortest path which the

roller can travel would be a straight line. This straight line can satisfy the requirements of the desired equations. The roller has to change direction when it goes from the return ramp to the power ramp. Figure 13 shows a schematic of a construction for the housing surface and roller. For the shortest path, the roller pivots about the edge of the two ramps and generates a circular path utilizing its own radius. The radius vector of this path from the rotor center is

$$\bar{r} = \bar{a} + \bar{b}$$

$\bar{a}$ is the roller radius and $\bar{b}$ is the fixed distance between the rotor center and the edge of the two ramps. The vectors are arranged as in Figure 14.

$$rR = b_x R - b_y P - a_x R + a_y P$$

$$= (b_x - a_x)R - (b_y - a_y)P$$

Multiplying by $\cdot P$,

$$b_y = a_y$$

$$a_x^2 = a^2 - a_y^2 = a^2 - b_y^2$$

$$rR = (b_x - \sqrt{a^2 - b_y^2})R - (b_y - a_y)P$$

Multiplying by $\cdot R$,

$$r = b_x - \sqrt{a^2 - b_y^2}$$

$$\bar{b} \cdot R = b_x = b \cos \theta$$

$$\bar{b} \cdot P = b_y = b \sin \theta$$

$$r = b \cos \theta - \sqrt{a^2 - b^2 \sin^2 \theta}$$

The roller enters the tangent angle for optimum torque and follows the path of a constant tangent angle, a constant torque, or a straight line. Due to the physical configuration, the roller radius, a, is also the stroking distance of the roller.

Let

$$d = \frac{a}{b}$$

$$r = b \cos \theta - \sqrt{d^2 b^2 - b^2 \sin^2 \theta}$$

$$r = b (\cos \theta - \sqrt{d^2 - \sin^2 \theta})$$

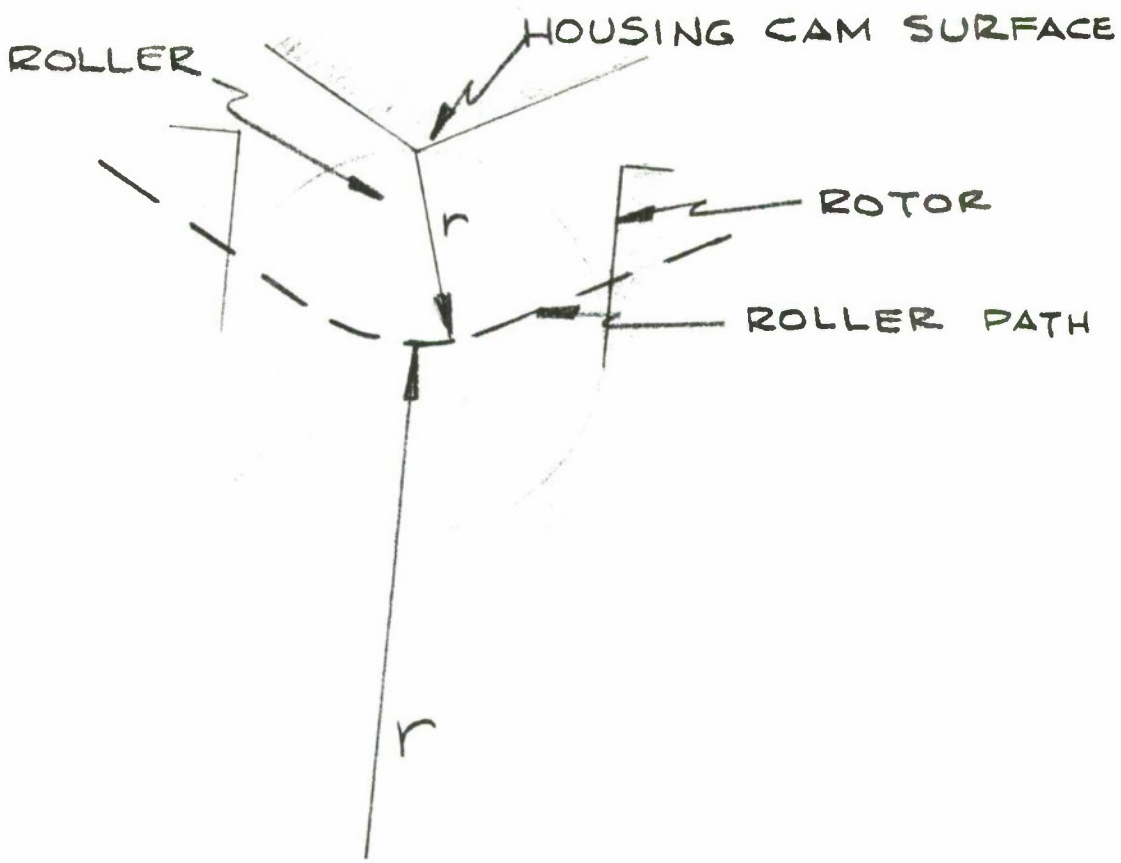

Figure 13. Roller Travel Path

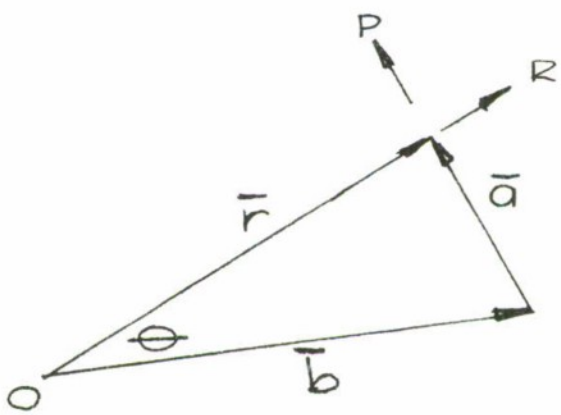

Figure 14. Components of the Radius Vector

The angle through which the rotor displaces in positioning the roller to the optimum tangent angle is

$$\tan (R,T) = \frac{r\dot{\theta}}{\dot{r}} = \sqrt{\frac{3mr\dot{\theta}^2}{F}}$$

$$\dot{r} = \frac{b\dot{\theta} \sin \theta}{\sqrt{d^2 - \sin^2 \theta}} \left(\cos \theta = \sqrt{d^2 - \sin^2 \theta}\right) = \frac{r\dot{\theta} \sin \theta}{\sqrt{d^2 - \sin^2 \theta}}$$

$$\frac{\sqrt{d^2 - \sin^2 \theta}}{\sin \theta} = \sqrt{\frac{3mr\dot{\theta}^2}{F}}$$

$$d^2 - \sin^2 \theta = \frac{3mr\dot{\theta}^2}{F} \sin^2 \theta$$

$$\sin \theta = \sqrt{d^2 - \frac{F}{3mr\dot{\theta}^2 + F}} \qquad (22)$$

In this equation, r can be considered as the initial radius distance between the rotor and roller centers at the beginning of the power stroke without introducing any appreciable error. This distance, $\dot{r}$, is the scalar quantity of b-a.

Past the initial phase, the path of the roller may take any path to continue the optimum torque condition. For this presentation, the straight line was chosen for two reasons. First, it is easier and more economical to fabricate; second, the acceleration in the normal direction is $(\dot{s}^2/\rho)N$. For a straight line, ρ is infinitely large and the acceleration scalar quantity in the N direction would become infinitely small or nonexistent. A force does remain in the normal direction - the housing-roller reaction - due to the fluid pressure. The radius vector for the optimum condition is the sum of the initial radius vector, $\bar{e}$, and the straight line path vector, $\bar{c}$.

$$\bar{r} = \bar{e} + \bar{c}$$

Utilizing i and j as unit vectors at right angles,

$$\bar{r} = ei + c_x i + c_y j$$

$$c_y = c_x \tan \alpha = (e + c_x) \tan \theta_2.$$

α is the angle for optimum torque.

$$c_x = e \frac{\sin \theta_2 \cos \alpha}{\sin (\alpha - \theta_2)}$$

$$c_y = e \frac{\sin \theta_2 \sin \alpha}{\sin (\alpha - \theta_2)}$$

$$r = e \sin \alpha \csc (\alpha - \theta_2)$$

$$e = b (\cos \theta_1 - \sqrt{d^2 - \sin^2 \theta_1})$$

$$\theta_2 = \theta - \theta_1$$

$$r = b (\cos \theta_1 - \sqrt{d^2 - \sin^2 \theta_1}) \sin \alpha \csc (\alpha + \theta_1 - \theta) \qquad (23)$$

If the roller continues on the straight line course to the end of the stroke and then abruptly changes direction, the acceleration force normal to the travel path would be infinitely large because ρ is zero.

$$\frac{\dot{s}^2}{0} N = \infty N$$

The minimum radius, ρ, with allowable tolerable normal load would have to be some finite length. If this length is equal to the radius of the roller, then the same ratio, d, can be utilized in the equation for the termination of the power stroke. The radius vector for the termination is the sum of the two vectors:

$$\bar{r} = \bar{e} + \bar{c}.$$

The scalar quantity of the radius vector is

$$r = b \left[(1 - d) \cos \beta + \sqrt{d^2 - (1 - d)^2 \sin^2 \beta} \right] \qquad (24)$$

β is the angle from top dead center.

Because of physical limitations, the roller has a pivot radius at the entrance of the power stroke equal to the roller radius. At the exit of the stroke, it also has a pivot radius to reduce the normal force. The shortest path between the two radii is a straight line tangent to both circles. The angle through which the rotor displaces in stroking the roller can be computed by two methods - graphically and mathematically. Of the two methods, the graphical is the faster and simpler. Figure 15 represents the graphic method.

Begin the graphical representation by drawing, to scale, the circle with the radius of rotor b about the center O. The length of this radius is selected by design requirements or by computation. After the number of rollers has been selected or computed, the ratio d equals a/b. (The roller radius, a, will be calculated from Equation 28.) Draw, to

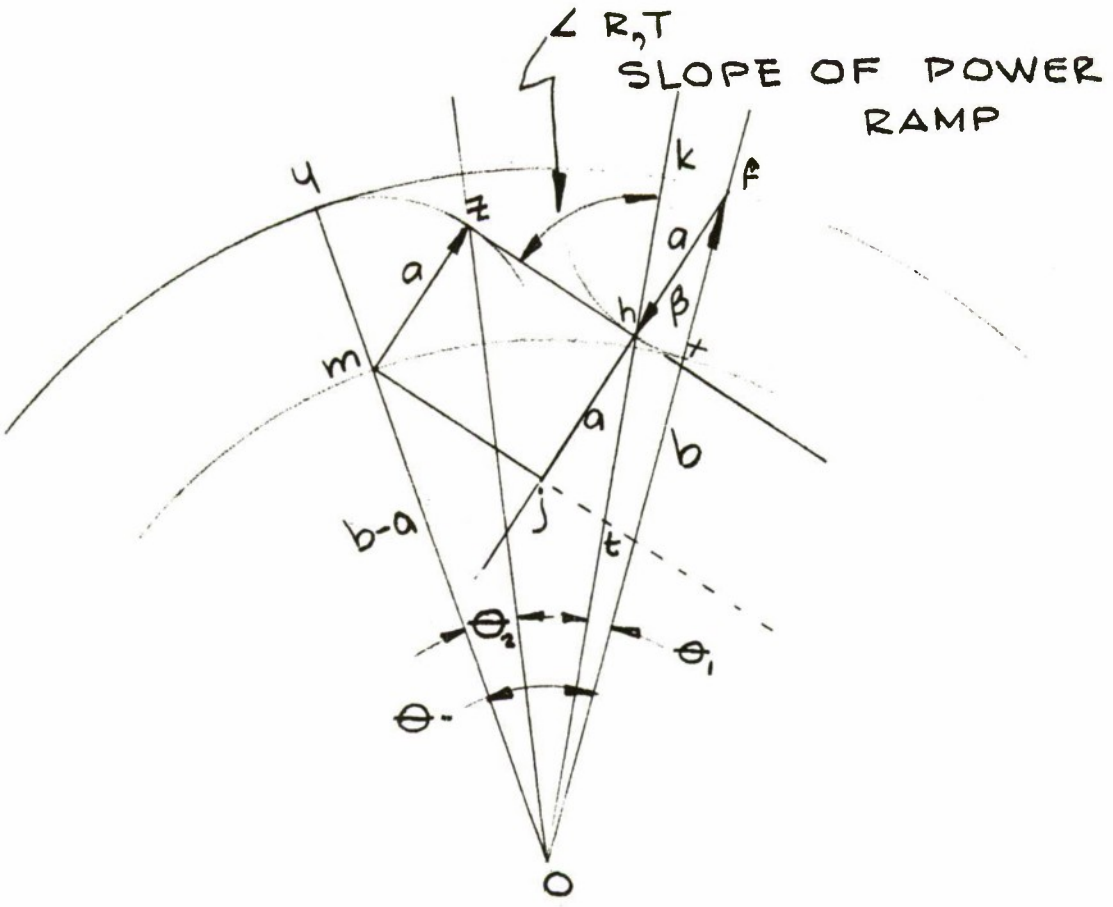

Figure 15. Graphical method of Determining the Rotor Power Displacement

scale, the circle with radius b-a. From the line O-f, measure the angle θ_1. This angle, f-O-k, is computed from Equation 22. Draw the circle a with its center at f, and it intersects the line O-k at h. Draw the line f-h to j. The length of the line f-j is the sum of the radii for the entrance and exit of the power stroke.

For this illustration, both radii were made equal, and the line f-j is 2a long. At the point j, draw a line perpendicular to the line f-j to the intersection of the circle with the radius b-a. The line f-O and the line O-m form the angle θ which the rotor displaces for the completion of the power stroke.

The analytical method is more involved, but it does give accurate results. The first step is to obtain the design requirements to compute the optimum torque and the ratio, d, of the roller radius to the rotor radius (Equations 22 and 28). Referring to Figure 15, b is the

rotor radius; a is the roller radius; θ is the rotor angular displacement; and θ_1 is the rotor displacement at the torque optimum condition. The distance

$$fm = \sqrt{b^2 + (b - a)^2 - 2b\,(b - a)\cos\theta}$$

$$= b\sqrt{1 + (1 - d)^2 - 2\,(1 - d)\cos\theta}.$$

Let $v = 1 - d$, and $b = 1$

$$fm = \sqrt{1 + v^2 - 2v\cos\theta}.$$

Also,

$$fm = \sqrt{(mj)^2 + (fj)^2}$$

$fj = 2a$, and $a = db$, $b = 1$;

$mj = mt - jt$.

$jt = fj \tan\beta$

$fj = 2a$, and $a = bd$, $b = 1$;

$jt = 2d \tan\beta$

$$mt = \sqrt{(Om)^2 + (Ot)^2 - 2(Om)(Ot)\cos\theta}$$

$Om = b - a = b(1 - d)$ and $b = 1$.

$Om = (1 - d) = v$.

$Ot = Of - ft$

$Of = b$, and $b = 1$;

$Of = 1$.

$ft = 2a \sec\beta$, $a = d$;

$ft = 2d \sec\beta$.

$Ot = 1 - 2d \sec\beta$.

Let $w = Ot = 1 - 2d \sec\beta$.

$$mt = \sqrt{v^2 + w^2 - 2vs\cos\theta}$$

$$mj = \sqrt{v^2 + w^2 - 2vw\cos\theta} - 2d \tan\beta$$

$$fm = \sqrt{(\sqrt{v^2 + w^2 - 2vw \cos\theta} - 2d \tan\beta)^2 + (2d)^2} = \sqrt{1 + v^2 - 2v \cos\theta}$$

$$(\sqrt{v^2 + w^2 - 2vw \cos\theta} - 2d \tan\beta)^2 + (2d)^2 = 1 + v^2 - 2v \cos\theta$$

$$\sqrt{v^2 + w^2 - 2vw \cos\theta} = \frac{w^2 + 2v \cos\theta\,(1 - w) + 4d^2 \sec^2\beta - 1}{4d \tan\beta}$$

$$\sqrt{v^2 + w^2 - 2wv \cos\theta} = \csc\beta\,(v \cos\theta - w)$$

$$v^2 \csc^2\beta \cos^2\theta - 2vw \cot^2\beta \cos\theta + w^2 \cot^2\beta - v^2 = 0$$

$$\cos\theta = \frac{1}{1 - d}\left\{\cos\beta\,(\cos\beta - 2d) \pm \sqrt{\left[1 - \cos^2\beta\right]\left[1 - \cos^2\beta - 3d^2 - 2d\,(1 - 2\cos\beta)\right]}\right\} \tag{25}$$

where $\beta = 90° - \left[\theta_1 - (R,T)\right]$.

The angle (R,T) is formed by the radial line and the tangent line.

$$\sec\beta = \frac{1}{\cos\beta}$$

$$\cos\beta = \cos\left\{90° - \left[\theta_1 + (R,T)\right]\right\} = \sin\left[\theta_1 + (R,T)\right]$$

$$\cos\beta = \sin\theta_1 \cos(R,T) + \cos\theta_1 \sin(R,T) \tag{26}$$

$$\tan(R,T) = \frac{r\dot{\theta}}{\dot{r}}$$

$$r = b\,(\cos\theta - \sqrt{d^2 - \sin^2\theta})$$

$$\dot{r} = r\dot{\theta}\,\frac{\sin\theta}{\sqrt{d^2 - \sin^2\theta}}$$

$$\tan(R,T) = \frac{\sqrt{d^2 - \sin^2\theta_1}}{\sin\theta_1} \tag{27}$$

$$\sin\theta_1 = d \cos(R,T) \tag{28}$$

$$\cos\theta_1 = \sqrt{1 - d^2 \cos^2(R,T)} \tag{29}$$

$$\cos \beta = d \cos^2 (R,T) + \sqrt{1 - d^2 \cos^2 (R,T)} \sin (R,T)$$

$$= d \cos^2 (R,T) + \sqrt{[1 - d^2 \cos^2 (R,T)][1 - \cos^2 (R,T)]}$$

$$\cos \beta = d \cos^2 (R,T) + \sqrt{(1 - d^2) + d^2[1 - \cos^2 (R,T)]^2} \qquad (30)$$

The angle, θ, which the rotor displaces for the complete stroking of the roller is at its minimum when the distance fm in Figure 15 is equal to the sum of the two radii. For this case,

$$\cos \frac{\theta}{2} = \sqrt{\frac{\frac{1}{4}[1 + (1 - d) + 2d][1 + (1 - d) + 2d - 4d]}{1 - d}}$$

$$= \sqrt{\frac{(2 + d)(2 - 3d)}{4(1 - d)}}$$

$$= \sqrt{\frac{1 + \cos \theta}{2}}$$

$$\cos \theta = \frac{(2 + d)(2 - 3d)}{2(1 - d)} - 1 \qquad (31)$$

For maximum rotor displacement, to completely stroke the roller, the line fm is perpendicular to the line Of.

$$\cos \theta = \frac{1 - 2d}{1 - d} \qquad (32)$$

From Figure 15, the roller path is xhzy. For a continuous torque, a roller should always be on the ramp hz, or a roller should be entering xh, while another should be exiting zy. This means that when a roller is at point z, another should be at point x. The rotor angular displacement for the roller to exit from the ramp is

$$\tan \theta_2 = \frac{d \sin (\angle ymz)}{(1 - d) + d \cos (\angle ymz)}$$

$$\angle ymz = \theta + \beta$$

$$\tan \theta_2 = \frac{d \sin (\theta + \beta)}{(1 - d) + d \cos (\theta + \beta)} \qquad (33)$$

The calculated horsepower is a function of the number of roller pistons and lobes in the system. For each roller, the work output is (Equation 14)

$$W = F(r_2 - r_1) - C.$$

r_2 is the longest radius distance that the center of the roller is from the shaft center; r_1 is the shortest radius distance; or $(r_2 - r_1)$ is the roller stroke distance. Due to the physical limitations, the maximum stroking of the roller is the roller radius, a.

$$r_2 - r_1 = a = bd \text{ (inches)}$$

On a per revolution basis, each roller will perform work with each cam in the housing. If there are n number of rollers and c number of cams in the housing, then the work per revolution is

$$W = Fanc - C$$

$$F = 2p\ell a$$

$$W = 2p\ell a^2 nc \tag{34}$$

The calculated horsepower is the work per revolution multiplied by the rotational speed and divided by the horsepower constant.

$$HP = \frac{W\ (RPM)}{396{,}000} = \frac{p\ell a^2 nc}{198{,}000}\ (RPM) \tag{35}$$

The ratio, d, of the roller radius, a, to the rotor radius, b, is made a function of the number, n, of rollers in the system.

$$a = \frac{b \sin (180°/n)}{1 + \sin (180°/n)}$$

$$d = \frac{a}{b} = \frac{\sin (180°/n)}{1 + \sin (180°/n)}$$

Allowing for a wall thickness of ten percent of the roller radius,

$$a = \frac{b \sin (180°/n)}{1.1 + \sin (180°/n)}$$

$$d = \frac{a}{b} = \frac{\sin (180°/n)}{1.1 + \sin (180°/n)}$$

The horsepower equation utilizes the parameters of the pressure, dimensions of the roller, and number of rollers and lobes. If the number and diameter of the rollers has been calculated from the horsepower equation, the rotor diameter can be calculated from:

$$b = a\left[\frac{1.1 + \sin (180°/n)}{\sin (180°/n)}\right] \tag{36}$$

and the ratio

$$d = \frac{a}{b} = \frac{\sin (180°/n)}{1.1 + \sin (180°/n)} \tag{37}$$

Equations 36 and 37 include a wall thickness between the slots in the rotor, which is ten percent of the roller radius.

By going one step further, the number of lobes can be made a function of the number of rollers. For working coordination of the rollers and lobes, the slope of the power ramp will be a function of the number of rollers; the other parameter, the rotational speed, becomes a function of the fluid pressure. The number of lobes can be one-half the number of rollers. If the number of rollers is an odd integer, the number of lobes becomes

$$c = \frac{n \pm 1}{2} \tag{38}$$

If the number of rollers is an even integer, the number of lobes becomes

$$c = \frac{n}{2} \pm 1 \tag{39}$$

If this numerical combination is employed, the mechanism will have a balanced functioning of the rollers, rotor, and lobes. When rollers enter the lobes simultaneously, the torque equation is multiplied by the number of rollers acting jointly. This joint action occurs when both integers are even and Equation 38 or 39 has been utilized.

APPENDIX B

EXPERIMENTAL TEST DATA

Pressurized Air (Cold Gas) Test

The pressurized air (cold gas) test was conducted 27 and 28 July 1965 in Building 316. Test instrumentation used consisted of: resistive load cell pressure pick-up, light detector pick-up, voltage amplifier, and oscillographs. Results of the test follow.

Generator		Motor		
Load Input (ohm)	Power Output (watt)	Rotational Speed (rpm)	Pressure Input[a] (psi)	Calculated Torque (in.-lb)
1/2	80.77	972	387	44.4
1/2	98.0	1138	403	50.1
1/2	49.3	1038	490	25.3
1/2	57.8	1050	503	29.2
1/2	95.4	1065	750	47.5
1/2	170.4	1050	758	86.5
1/2	158.5	1140	758	74.4
1/2	183.2	1272	786	75.6
1/2	204.6	1236	990	87.5
1/2	259.3	1320	1070	104.0
1	46.3	822	370	29.7
1	94.6	960	392	52
1	121	960	792	67.2
1	214.7	1128	792	101
1	170.4	1050	758	86.5
1	240	1140	1050	112
1	297.5	1230	1100	128
2-1/2	191.5	1185	770	90.5
2-1/2	222.5	1200	810	98.0
2-1/2	217.2	1140	970	101
2-1/2	239.2	1230	1050	103.8
5	22.5	750	305	15.9
5	31.3	780	335	21.4
5	175	1230	780	72.2
5	202	1305	830	82.1
5	202	1275	946	84.3
5	230	1380	1020	88.9

[a]Compressed air.

Generator		Motor		
Load Input (ohm)	Power Output (watt)	Rotational Speed (rpm)	Pressure Input[a] (psi)	Calculated Torque (in.-lb)
10	35.0	825	350	22.6
10	75.7	720	376	55.8
10	130.8	1230	806	56.8
10	144.0	1320	840	58
15	26.3	786	320	17.8
15	38.9	870	332	23.6
15	175	1440	828	53.5
15	193	1500	876	68.2

[a]Compressed air.

Ballistic Test
(Hot Gas Generator to Motor)

The hot gas test was conducted 3 August 1965. Motion picture coverage was made of each test for record and back-up check on the instrumentation. Results follow.

	Pressure (psi)		Output	
Test	Generator	Motor Intake	Motor	Generator
First	1710	520	NR[a]	NR[a]
Second	1703	520	10 revolutions	NR[a]

[a]Instrumentation uncalibrated but, since it was moved prior to actual running of tests, it lost its effectiveness on recordings.

DISTRIBUTION

Hq, U.S. Army Materiel Command
Washington, D. C. 20315

1 Attn: Chief Scientist, AMCSA-SC

1 Attn: Mr. N. L. Klein

2 Attn: Mr. J. Kaufman

Hq, U.S. Army Munitions Command
Dover, N. J. 07801

1 Attn: Technical Information Div

1 Attn: Dr. J. V. R. Kauffman

3 Attn: Dr. J. Erway, Research Br

1 Attn: Mr. M. H. Stratton, RDT&E
Progress Br., AMSMU-CO-R

1 Attn: AMSMU-LA, AF Liaison Officer

1 Attn: AMSMU-LC, CDC Liaison Off.

1 Attn: AMSMU-LM, USMC Liaision Off.

Army Research Office
Physical Sciences Division
Attn: Dr. I. R. Hershner
3045 Columbia Pike
Arlington, Va. 22204

Commanding Officer
Watervliet Arsenal
Watervliet, N. Y. 12189

1 Attn: Dr. F. K. Sautter

1 Attn: Lt. M. J. Hordon

1 Attn: Dr. R. E. Weigle

Commanding Officer
Detroit Arsenal
Warren, Mich. 48090

Commanding Officer
Rock Island Arsenal
Rock Island, Ill. 61202

1 Attn: Dr. Hansen

1 Attn: Mr. S. Eisler

Commanding Officer
Picatinny Arsenal
Dover, N. J. 07801

1 Attn: Mr. L. Ericson

1 Attn: L. W. Doremus

1 Attn: Dr. H. Matsugama

U.S.Army Chemical Research and
Development Laboratories
Attn: Dr. C. M. Herget
Asst Tech Director for Research
Edgewood Arsenal, Md. 21010

Commanding Officer
Harr Diamond Laboratories
Washington, D. C. 20438

1 Attn: Mr. C. Swenk

1 Attn: AMXDO-TIB

Institute for Exploratory Research
Signal Laboratory
Fort Monmouth, N. J. 07703

1 Attn: Dr. Horst Kedesdy,
Dir, Exploratory Res, Div E.

1 Attn: Dir, Exploratory Res, Div S

Commanding Officer
Ballistic Research Laboratory
Aberdeen Proving Ground, Md. 21005

1 Attn: Dr. E. Minor

1 Attn: Dr. Curtis Lampson

Hq, U.S. Army Materiel Research Agency
Watertown Arsenal
Watertown, Mass. 02172

1 Attn: Technical Information Center

1 Attn: George Darcy
Prog & Tech Div.

1 Attn: Dr. L. S. Foster
Atomic Energy Program

1 Attn: Dr. H. Priest
Basic Research Laboratory

1 Attn: Mr. J. Jacobson

Commanding Officer
U.S. Army Research Office-Durham
Box CM, Duke Station
Durham, N. C. 27706

1 Attn: Commanding Officer

1 Attn: Dr. J. Dawson

1 Attn: Mr. J. Lane

1 Attn: Mr. G. Cox

1 Attn: Dr. H. Robl

1 Attn: Dr. G. Mace

1 Attn: Dr. G. Wyman

Dr. R. M. Thomson
Advances Research Projects Agency
Department of Defense
Washington, D. C. 20301

National Aeronautics & Space Adm
Attn: Dr. B. G. Achhammer
Materials Division
1540 H St., N.W.
Washington, D. C. 20546

NASA, Ames Research Center
Attn: Theoretical Branch
Moffett Field, Calif.

Hq, Aeronauticql Systems Division
Attn: Information Processing Section
Christine Jackson
Wright-Patterson AFB, Ohio 45433

Defense Documentation Center (20)
Cameron Station
Alexandria, Va. 22314

Dr. Wm. Boghosian
Moore School of Electrical Engr.
University of Pennsylvania
Philadelphia, Pa. 19104

Dr. Max Caspari
Physics Dept
University of Pennsylvania
Philadelphia, Pa. 19104

Dr. Louis Girifalco
Laboratory for Research on the
Structure of Matter,
University of Pennsylvania
Philadelphia, Pa. 19104

Dr. J. Hobstetter
Dr, Laboratory for Research on the
Structure of Matter
University of Pennsylvania
Philadelphia, Pa. 19104

Dr. Cassius Curtis
Department of Physics
Lehigh University
Bethlehem, Pa.

Dr. Leonard Muldawer
Department of Physics
Temple University
Philadelphia, Pa. 19122

Dr. Elmer Offenbacher
Department of Physics
Temple University
Philadelphia, Pa. 19122

Dr. Robert E. Salomon
Department of Chemistry
Temple University
Philadelphia, Pa. 19122

Dr. Hans Johassen
Department of Chemistry
Tulane University
New Orleans 15, La.

Dr. Herbert Muether
Stonybrook, N. Y.

Dr. Gilbert Manns, Chairman
Department of Chemistry
University of Detroit
Detroit, Mich.

Dr. Thomas A. Read, Chairman
Dept of Mining & Metallurgical Engr
University of Illinois
Urbana, Ill.

Dr. Paul Levy
Brookhaven National Laboratories
Associated Universities, Inc.
Upton, Long Island, N. Y. 11973

Reproduction Branch
FRANKFORD ARSENAL
Philadelphia, Pa.
Date Printed:
7-5-66

UNCLASSIFIED

Security Classification

DOCUMENT CONTROL DATA - R&D

(Security classification of title, body of abstract and indexing annotation must be entered when the overall report is classified)

1. ORIGINATING ACTIVITY *(Corporate author)*

FRANKFORD ARSENAL, Philadelphia, Pa. 19137

(ATTN: SMUFA L3300)

2a. REPORT SECURITY CLASSIFICATION

Unclassified

2b GROUP

NA

3. REPORT TITLE

NEW FUNDAMENTAL MECHANISM FOR AN ENERGY CONVERSION DEVICE

4. DESCRIPTIVE NOTES *(Type of report and inclusive dates)*

Technical Research Report - 1 Jul 62 to 31 July 1965.

5. AUTHOR(S) *(Last name, first name, initial)*

PISANO, Frank T.

6. REPORT DATE	7a. TOTAL NO. OF PAGES	7b. NO. OF REFS
April 1966	51	None

8a. CONTRACT OR GRANT NO.	9a. ORIGINATOR'S REPORT NUMBER(S)
AMCS Code 5010.11.844	FA Report R-1812
b. PROJECT NO.	
c.	9b. OTHER REPORT NO(S) *(Any other numbers that may be assigned this report)*
d.	

10. AVAILABILITY/LIMITATION NOTICES

Distribution of this report is unlimited.

11. SUPPLEMENTARY NOTES	12. SPONSORING MILITARY ACTIVITY
	Frankford Arsenal - In-house initiated R&D

13. ABSTRACT

This report summarizes the theoretical and experimental studies conducted on a hot gas motor, a fundamentally new mechanism, as an energy conversion device.

In the theoretical study, the relationship of the working components was determined and optimized for maximum converison of fluid potential and kinetic energy into useful mechanical work. A test model of the hot gas motor was fabricated and a limited series of test runs was conducted, using both cold and hot gas.

This report also presents a design discusssion, a vector analysis, and test data of this novel motor.

DD FORM 1 JAN 64 1473

UNCLASSIFIED

Security Classification

14. KEY WORDS	LINK A		LINK B		LINK C	
	ROLE	WT	ROLE	WT	ROLE	WT
Propellant Actuated Device Motor Hydraulic Mechanism Pneumatic Mechanism						

INSTRUCTIONS

1. ORIGINATING ACTIVITY: Enter the name and address of the contractor, subcontractor, grantee, Department of Defense activity or other organization *(corporate author)* issuing the report.

2*a*. REPORT SECURITY CLASSIFICATION: Enter the overall security classification of the report. Indicate whether "Restricted Data" is included. Marking is to be in accordance with appropriate security regulations.

2*b*. GROUP: Automatic downgrading is specified in DoD Directive 5200.10 and Armed Forces Industrial Manual. Enter the group number. Also, when applicable, show that optional markings have been used for Group 3 and Group 4 as authorized.

3. REPORT TITLE: Enter the complete report title in all capital letters. Titles in all cases should be unclassified. If a meaningful title cannot be selected without classification, show title classification in all capitals in parenthesis immediately following the title.

4. DESCRIPTIVE NOTES: If appropriate, enter the type of report, e.g., interim, progress, summary, annual, or final. Give the inclusive dates when a specific reporting period is covered.

5. AUTHOR(S): Enter the name(s) of author(s) as shown on or in the report. Enter last name, first name, middle initial. If military, show rank and branch of service. The name of the principal author is an absolute minimum requirement.

6. REPORT DATE: Enter the date of the report as day, month, year; or month, year. If more than one date appears on the report, use date of publication.

7*a*. TOTAL NUMBER OF PAGES: The total page count should follow normal pagination procedures, i.e., enter the number of pages containing information.

7*b*. NUMBER OF REFERENCES: Enter the total number of references cited in the report.

8*a*. CONTRACT OR GRANT NUMBER: If appropriate, enter the applicable number of the contract or grant under which the report was written.

8*b*, 8*c*, & 8*d*. PROJECT NUMBER: Enter the appropriate military department identification, such as project number, subproject number, system numbers, task number, etc.

9*a*. ORIGINATOR'S REPORT NUMBER(S): Enter the official report number by which the document will be identified and controlled by the originating activity. This number must be unique to this report.

9*b*. OTHER REPORT NUMBER(S): If the report has been assigned any other report numbers *(either by the originator or by the sponsor)*, also enter this number(s).

10. AVAILABILITY/LIMITATION NOTICES: Enter any limitations on further dissemination of the report, other than those imposed by security classification, using standard statements such as:

(1) "Qualified requesters may obtain copies of this report from DDC."

(2) "Foreign announcement and dissemination of this report by DDC is not authorized."

(3) "U. S. Government agencies may obtain copies of this report directly from DDC. Other qualified DDC users shall request through _____."

(4) "U. S. military agencies may obtain copies of this report directly from DDC. Other qualified users shall request through _____."

(5) "All distribution of this report is controlled. Qualified DDC users shall request through _____."

If the report has been furnished to the Office of Technical Services, Department of Commerce, for sale to the public, indicate this fact and enter the price, if known.

11. SUPPLEMENTARY NOTES: Use for additional explanatory notes.

12. SPONSORING MILITARY ACTIVITY: Enter the name of the departmental project office or laboratory sponsoring *(paying for)* the research and development. Include address.

13. ABSTRACT: Enter an abstract giving a brief and factual summary of the document indicative of the report, even though it may also appear elsewhere in the body of the technical report. If additional space is required, a continuation sheet shall be attached.

It is highly desirable that the abstract of classified reports be unclassified. Each paragraph of the abstract shall end with an indication of the military security classification of the information in the paragraph, represented as *(TS)*, *(S)*, *(C)*, or *(U)*.

There is no limitation on the length of the abstract. However, the suggested length is from 150 to 225 words.

14. KEY WORDS: Key words are technically meaningful terms or short phrases that characterize a report and may be used as index entries for cataloging the report. Key words must be selected so that no security classification is required. Identifiers, such as equipment model designation, trade name, military project code name, geographic location, may be used as key words but will be followed by an indication of technical context. The assignment of links, rules, and weights is optional.